Correction of deposit ages for inherited ages of charcoal: implications for sediment dynamics inferred from random sampling of deposits on headwater valley floors

Citation	Frueh, W. T., & Lancaster, S. T. (2014). Correction of deposit ages for inherited ages of charcoal: implications for sediment dynamics inferred from random sampling of deposits on headwater valley floors. Quaternary Science Reviews, 88, 110-124. doi:10.1016/j.quascirev.2013.10.029
DOI	10.1016/j.quascirev.2013.10.029
Publisher	Elsevier
Version	Accepted Manuscript
Terms of Use	http://cdss.library.oregonstate.edu/sa-termsofuse

Quaternary Science Reviews 88 (2014) 110–124

Contents lists available at ScienceDirect

Quaternary Science Reviews

journal homepage: www.elsevier.com/locate/quascirev

Correction of deposit ages for inherited ages of charcoal: implications for sediment dynamics inferred from random sampling of deposits on headwater valley floors

W. Terry Frueh[a,b], Stephen T. Lancaster[a,c,*]

[a] College of Earth, Ocean, and Atmospheric Sciences, Oregon State University, Corvallis, Oregon, USA.
[b] Oregon Department of Forestry, Salem, Oregon, USA
[c] Institute for Water and Watersheds, Oregon State University, Corvallis, Oregon, USA.

ARTICLE INFO

Article history:
Received 18 May 2013
Received in revised form
27 October 2013
Accepted 28 October 2013
Available online

Keywords:
Radiocarbon dating
Age correction
Geomorphology
Sediment
Reservoir theory
Oregon Coast Range

ABSTRACT

Inherited age is defined herein as the difference between times of carbon fixation in a material and deposition of that material within sediments from which it is eventually sampled in order to estimate deposit age via radiocarbon dating. Inheritance generally leads to over-estimation of the age by an unknown amount and therefore represents unquantified bias and uncertainty that could potentially lead to erroneous inferences. Inherited ages in charcoal are likely to be larger, and therefore detectable relative to analytic error, where forests are dominated by longer-lived trees, material is stored for longer periods upslope, and downstream post-fire delivery of that material is dominated by mass movements, such as in the near-coastal mountains of northwestern North America. Inherited age distribution functions were estimated from radiocarbon dating of 126 charcoal pieces from 14 stream-bank exposures of debris-flow deposits, fluvial fines, and fluvial gravels along a headwater stream in the southern Oregon Coast Range, USA. In the region, these 3 facies are representative of the nearly continuous coalescing fan-fill complexes blanketing valley floors of headwater streams where the dominant transport mechanism shifts from debris-flow to fluvial. Within each depositional unit, and for each charcoal piece within that unit, convolution of the calibrated age distribution with that of the youngest piece yielded an inherited age distribution for the unit. Fits to the normalized sums of inherited age distributions for units of like facies provided estimates of facies-specific inherited age distribution functions. Finally, convolution of these distribution functions with calibrated deposit age distributions yielded corrections to published valley-floor deposit ages and residence time distributions from nearby similar sites. Residence time distributions were inferred from the normalized sums of distributions of ~ 30 deposit ages at each of 4 sites: 2 adjacent valley reaches ~ 10^3 m long and within ~ 10^2 m of 2 tributary confluences. Mean inherited ages from the observed distributions are 666, 688, and 1506 yr for debris-flow deposits, fluvial fines, and fluvial gravels, respectively. On average, correction reduced estimates of individual deposit age means by a factor of 0.71 (0.56–0.94) and increased standard deviations by a factor of 6.1 (0.97–43). Across sites, mean residence times decreased by 24.0% and standard deviations by 12.5% on average. Corrected residence time distributions have thicker tails, as indicated by gamma-distribution fits with smaller shape factors, and these changes are significant relative to the bootstrapped 95% confidence limits representing potential error in the sampling for inherited ages. The ratio of the means of sediment age and residence time ranged from 1.03 to 1.80 across sites before correction and 1.21 to 2.18 after correction, where a value of one implies that probability of evacuation from the "reservoir" comprising valley-floor deposits is independent of time since deposition. Corrected values of this ratio therefore indicate that evacuation favors younger deposits at all sites, whereas uncorrected results implied age-independent evacuation from the more downstream valley reach.

1. Introduction

Radiocarbon dating of organic material is often used to estimate the age of the sediment deposits in which the material is found (e.g., Bush and Stillman, 2007; Personius et al., 1993; Pierce and Meyer, 2008), but an accurate estimate based solely on radiocarbon dating assumes that the dated material was young, i.e., had effectively zero age, at the time of deposition. Two kinds of cases violate this assumption: 1) the material was not incorporated into a deposit shortly after carbon fixation; and 2) the material remained, for an extended period of time, in storage on its journey from its source to a particular deposit (e.g., Blong and Gillespie, 1978).

In radiocarbon dating, and consistently herein, age is effectively treated as a random variable, T, with a probability density function (PDF), $f_T(t)$, that incorporates uncertainties in both radiocarbon concentration in the dated material and the calibra-

*Corresponding author. College of Earth, Ocean, and Atmospheric Sciences, Oregon State University, Corvallis, Oregon, USA.
Email addresses: tfrueh@odf.state.or.us (W. Terry Frueh), lancasts@geo.oregonstate.edu (Stephen T. Lancaster)

Author-prepared copy of article published in *Quaternary Science Reviews* http://dx.doi.org/10.1016/j.quascirev.2013.10.029.

tion curve relating radiocarbon concentration to calendar age. The expected value of age is the mean, $\overline{T} = \int_{-\infty}^{\infty}[t f_T(t)]\mathrm{d}t$, sometimes called the "weighted mean," where the PDF is the weighting function (Telford et al., 2004). Uncertainty is expressed in terms of the standard deviation, or the square-root of the variance, $\sigma_T^2 = \int_{-\infty}^{\infty}[(t-\overline{T})^2 f_T(t)]\mathrm{d}t$. In this paper, we explicitly incorporate uncertainties due to violations of the zero-age assumption and determine whether these uncertainties significantly affect, on the one hand, age estimates and uncertainties associated with individual samples of organic material and, on the other hand, inferences of system behavior (in this case, geomorphic) based on many samples.

Some definitions are necessary to draw distinctions among the various "ages" and "times" considered herein. "Sample age" is the time between carbon fixation within and radiocarbon dating of a sample of organic material, typically charcoal or wood. "Deposit age" is the time since deposition of the sediment in a unit or stratum from which a sample is taken for radiocarbon dating. "Inherited age" is the time between carbon fixation within a sample and its deposition within the unit to be dated and is equivalent, at least conceptually, to the difference between sample age and deposit age. Inherited age includes "inbuilt age," which Gavin (2001) defined as the time between carbon fixation and charcoal formation. Geomorphologists have used deposit ages, e.g., of bank exposures, to infer sediment residence times, where "sediment residence time," or simply "residence time," is the time between deposition and evacuation of sediment and is also known as "transit time" or "storage time." System characteristics determine the residence time distribution and its moments (e.g., mean, variance), and to a limited extent, vice versa. In particular, the residence time distribution implies the distribution of "sediment age." Like deposit age, sediment age is defined as the time since deposition but is used here in the context of a probability distribution for all sediments within a "reservoir," i.e., a control volume in which sediment may be stored, such as an alluvial fan. Similarly, residence time is used in the context of sediments leaving a reservoir (Bolin and Rodhe, 1973; Eriksson, 1971; Dietrich et al., 1982; Lancaster and Casebeer, 2007; Lancaster et al., 2010; Bradley and Tucker, 2013).

After Aubry et al. (2009), we report durations with the unit of "year," or "yr" (or "kyr" for "thousands of years") and dates relative to the present with the unit of "annus," or "a" (or "ka" for "thousands of years before present"). Sample ages are reported as dates in calibrated or radiocarbon years relative to AD 1950 ("a BP" or "^{14}C a BP," respectively). Deposit ages, inherited ages, residence times, and sediment ages are reported as durations. Inherited ages require no reference datum, but the others are inferred from ages relative to the time of sampling.

Magnitudes of inherited ages and, thus, the biases inherent in many deposit age estimates are generally unknown and therefore not systematically accounted for. Blong and Gillespie (1978) found inherited ages of bulk charcoal samples from a river bed in coastal New South Wales as great as 1500 ^{14}C yr and therefore regarded any single sample age as a "maximum" deposit age, i.e., an age estimate that may be larger than the actual age by an unknown amount. Stratigraphic age control can constrain these magnitudes, essentially revealing cases in which inherited ages are large enough to cause age inversions (i.e., stratigraphically higher samples yielding greater ages than lower samples). For example, in 7 sites with stratigraphic age control, Lancaster and Casebeer (2007) and Lancaster et al. (2010) found 3 age inversions of 455, 976, and 3909 yr in headwater valleys of the Oregon Coast Range. Dating of multiple samples and assuming that the actual deposit age is equal to the minimum of the sample ages can reduce error, but again, that error is not well described (e.g., Akciz et al., 2009; Meyer et al., 1995; Tornqvist et al., 1992). Moreover, the necessary number of samples may make this method impractically large. Based on differences between timing of fire events inferred from dating of soil charcoal and counts of tree rings on the west side of Vancouver Island, Gavin (2001) found that only 3 of 26 samples had inbuilt ages less than 150 yr, whereas the median and maximum were 270 yr and 670 yr, respectively. Gavin et al. (2003) incorporated this uncertainty by a convolution of the distribution of inbuilt ages with calibrated age distributions, but his method required independent determination of the true times of the types of events in question, information that may be unobtainable in many cases, such as with the timing of ordinary fluvial deposition.

The events leading to charcoal deposition in valley-floor sampling sites may form lengthy histories: After radiocarbon is fixed in new woody material by organisms (i.e., trees), those organisms may live for many years before dying, and that death may precede burning and, hence, charcoal production by additional years. Moreover, decay may expose older interior wood, which may then be susceptible to burning during fires (Gavin, 2001). Charcoal may then remain on dead tree trunks for some time before falling, after which the charcoal on hillslopes may be incorporated into mobile regolith, which will, after some time, work its way downslope and into areas prone to erosion by overland flow or mass movement, where that charcoal may remain for many years before moving downslope with eroded sediment, often via debris flow, and into channel networks. Charcoal pieces may then stay in one or more valley-floor deposits for many years before finally coming to rest in the fluvial or debris-flow deposits from which we take samples for radiocarbon dating (Nichols et al., 2000). Or, the times between these effectively stochastic events may be short enough that inherited ages are negligibly short.

In the absence of appropriate site-specific data, uncertainty with respect to deposit ages is nearly unbounded. For example, Lancaster et al. (2010) found charcoal samples with mean calibrated ages of 16.6 ka BP, 148 a BP, and 168 a BP, from bottom to top, in an otherwise unremarkable stream bank in the Oregon Coast Range. The upper samples provide effectively no constraint on the inherited age of the lowest.

The accuracy of statistics assembled from many samples may be more important than, but just as uncertain as, the accuracy of any one deposit age. For example, using reservoir theory and large numbers of ages of deposits exposed in stream banks as proxies for residence times, Lancaster and Casebeer (2007) and Lancaster et al. (2010) inferred sediment flux rates and relative probabilities of valley-floor sediment evacuation as a function of sediment age. According to reservoir theory, if residence times are exponentially distributed, mean residence times are equivalent to mean sediment ages, and evacuation probability is invariant with respect to sediment age. In contrast, if residence time probabilities decrease more slowly with time (i.e., have thicker tails) than an exponential distribution, then mean residence times are less than mean sediment ages for the entire reservoir, and evacuation probability decreases with sediment age (Bolin and Rodhe, 1973; Dietrich et al., 1982; Eriksson, 1971; Lancaster and Casebeer, 2007; Lancaster et al., 2010). Substantial inherited ages in the systems studied by Lancaster and Casebeer (2007) and Lancaster et al. (2010) might have implications far beyond the correct characterization of sediment routing in the southern Oregon Coast Range, and even of geomorphic processes more generally, and could suggest reinterpretation of a broad range of studies using radiocarbon dating to estimate deposit ages.

In the Oregon Coast Range in particular, large trees and episodic hillslope erosion by mass movement may lead to substantial inherited ages, so sites in this region may provide a large and readily

characterized inherited age "signal" relative to the "noise" of well-established uncertainties inherent in radiocarbon dating. However, other factors may tend to make inherited ages small: Fires mainly burn the extremities and exteriors of the trees, i.e., the youngest parts of live trees (Gavin, 2001; Scott, 2010; Spies et al., 1988), and post-fire sediment transport may be greatly accelerated on hillslopes that are typically steeper than the angle of repose (Jackson and Roering, 2009; Roering and Gerber, 2005).

The specific objective of this study is to characterize inherited ages, in both average magnitude and their distribution, to address these questions: 1) How greatly do inherited ages alter measured deposit ages and, hence, inferred quantities such as residence times, sediment ages, and sediment fluxes in sediment reservoirs comprising deposits adjacent to small streams of the Oregon Coast Range? 2) How does inherited age bias affect measured sediment residence time distributions and, hence, inferred sediment reservoir dynamics in these streams?

More generally, we present a suite of generally applicable methods of inherited age estimation and deposit age correction. We estimate distributions of inherited ages from multiple charcoal sample ages taken from units representing debris-flow, fine fluvial, and coarse fluvial deposit types, or facies. We use these distributions to correct measured deposit ages and assess the effects of correction on both the deposit age distributions based on individual samples and the residence time distributions based on many samples. Finally, we estimate the uncertainties in distributions of inherited ages and corrected residence times due to possible sampling error in the estimation of inherited ages.

2. Study Areas in the Oregon Coast Range

The climate of the mountainous rain forests of northwestern North America is typified by long rainy seasons of low-intensity rainfall rarely accompanied by lightning, and these conditions lead to infrequent fires, large, long-lived trees, and abundant charcoal for radiocarbon dating. Sites for the current study fall within the *Tsuga heterophylla* Sarg. (western hemlock) zone in the Oregon Coast Range. Mean annual rainfall is 2.3 m, with 93% of that falling from October to May, and only 2% in July and August (Western Regional Climate Center, 2013). Western hemlock is the climax species, but Douglas-fir [*Pseudotsuga menziesii* (Mirb.) Franco] typically dominates live biomass for up to 1000 yr after forest-killing fire, and trunk diameters can reach 3 m (Franklin and Dyrness, 1973; Franklin and Hemstrom, 1981; Pabst et al., 2008). A third large conifer, western redcedar (*Thuja plicata* Donn ex D. Don), may produce snags (i.e., standing dead trees) that are an order of magnitude more resistant to decay (Daniels et al., 1997; Gavin, 2001), although inter-species differences measured for fallen wood are small (Sollins et al., 1987). At the Oregon Coast Range sites of Lancaster et al. (2010), 75% of identifiable charcoal pieces were Douglas-fir, so its dominance apparently extends through charcoal production, transport, and preservation.

Douglas-fir lifespans may contribute substantially to inherited ages, but probably less than at the western Vancouver Island sites of Gavin (2001), where annual precipitation is greater (3.5 m) and western redcedar more common (Gavin, 2001). The mortality rate of Douglas-fir in the Oregon Coast Range is greater than that of western redcedar on western Vancouver Island by perhaps a factor of 2.1, if the relative rates are inversely proportional to annual precipitation, and lifespans will differ by the inverse factor (Pabst et al., 2008).

Charcoal, at least in part, moves and deposits with the sediment. Typical living and dead biomasses of $\lesssim 50$ kg/m^2 and $\lesssim 80$ kg/m^2, respectively, and fires with average return intervals of $\sim$ 200 yr

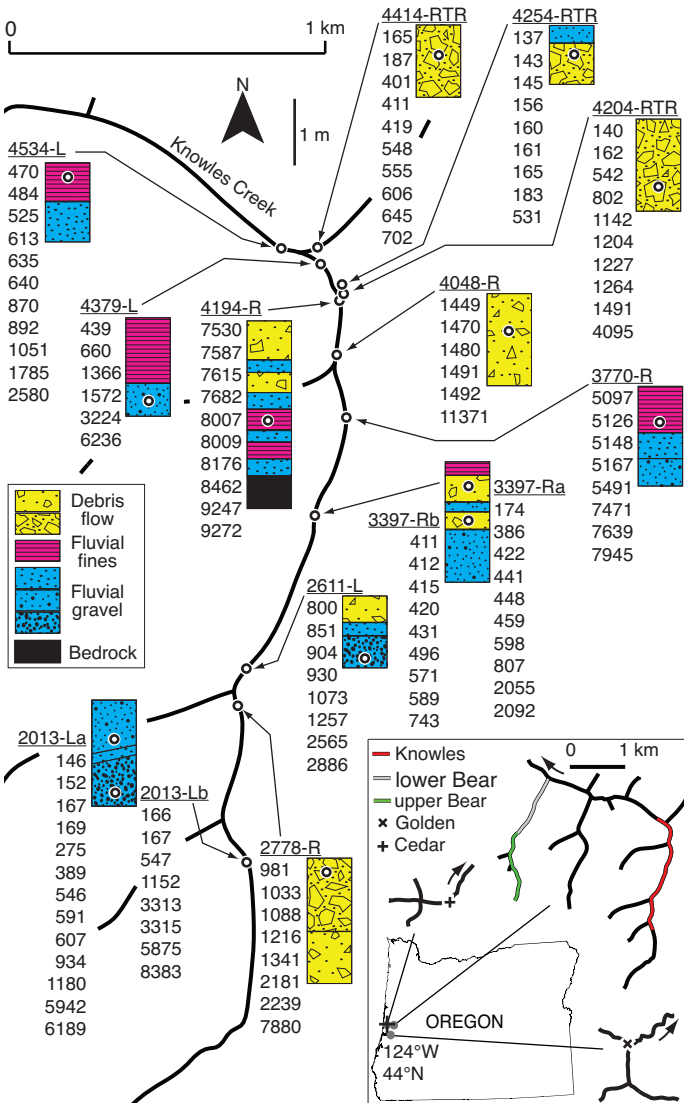

Fig. 1. Map of Knowles Creek sample site locations (white circles) in plan view and within stratigraphic columns of channel banks; depositional units (underlined text) identified by stream-wise distance from divide (m), right (R) or left (L) stream bank (facing downstream) or right bank of right-bank tributary (RTR), and upper (a) or lower (b) unit in stratigraphic column; and mean calibrated sample ages, from youngest to oldest, in years before AD 1950 (a BP) of charcoal extracted from respective units. Darker and lighter shades of yellow, red, and blue differentiate coarser and finer textures of debris-flow deposits, fluvial fines, and fluvial gravels, respectively. Horizontal scale bar applies to stream map, and vertical bar to stratigraphic columns. Inset: Channel networks at sampled sites (black), with sampled reaches of Knowles and Bear Creeks (non-black) and tributary confluence sites on Cedar and Golden Ridge Creeks (symbols), shown with respect to locations (gray circles) in state of Oregon, USA, with downstream directions indicated by arrows.

produce $\lesssim 0.005$ kg/m^2/yr of charcoal, or $\lesssim 3\%$ by weight of the total sediment yield, great enough that availability of charcoal did not influence the selection of sampling locations for the studies of Lancaster and Casebeer (2007) and Lancaster et al. (2010) (Anderson et al., 2002; Blackard et al., 2008; Gavin, 2001; Heimsath et al., 2001; Lancaster and Casebeer, 2007; Lancaster et al., 2010; Long et al., 1998; Spies et al., 1988).

The coastal ranges of the Pacific Northwest are also characterized by active rock uplift that, with the mild climate, produces steep slopes (Tucker and Bras, 2000; Tucker, 2004). For soils derived from the massive sandstone and interbedded mudstone of the Eocene Tyee Formation in the Oregon Coast Range, slope angles typically exceed the angle of repose on hillslopes and even

Table 1
Site and reservoir characteristics[a].

		Lower Bear	Upper Bear	Cedar fan	Golden Ridge trib.
Area (km^2)		2.23 (0.88)[b]	1.35	0.14	1.5
Gradient (%)		2–5	5–25	9.8	4.8
Volume (m^3)		4.72×10^4	2.23×10^4	$2.4–3.6 \times 10^4$	3200
Length (m)		1300	1300	130	38
Residence	$\overline{T_r}$	979 [951, 1030] (1300)	256 [248, 274] (361)	1140 [1100, 1180] (1370)	1220 [1160, 1290] (1630)
Time (yr):	σ_{T_r}	1160 [1130, 1210] (1340)	442 [429, 463] (533)	2090 [2030, 2130] (2210)	1760 [1690, 1860] (2050)
	T_{r50}	428 [413, 473] (723)	108 [103, 123] (208)	311 [301, 326] (556)	506 [486, 536] (811)
	T_{r90}	2780 [2700, 2920] (3530)	613 [598, 643] (738)	2990 [2880, 3080] (3390)	4900 [4550, 5240] (5800)
Sediment	$\overline{T_a}$	1180 (1340)	504 (572)	2480 (2460)	1880 (2100)
age (yr):	σ_{T_a}	1050 (1160)	557 (612)	2600 (2630)	1730 (1910)
	T_{a50}	888 (1030)	288 (343)	1530 (1490)	1340 (1430)
	T_{a90}	2750 (3080)	1450 (1570)	6720 (6710)	4630 (5130)
Flux (kg/yr)		6.07×10^4 (4.54×10^4)	1.10×10^5 (7.78×10^4)	$2.7–4.0 \times 10^4$ ($2.2–3.3 \times 10^4$)	3300 (2500)
Efficiency (%)		15.4 (11.6)[c]	30.6 (21.7)	71–110 (59–89)	0.83 (0.62)

[a] Contributing basin area, channel gradient, reservoir sediment volume, combined channel length, residence time, sediment age, mass flux through the reservoir, and reservoir efficiency for the lower and upper Bear Creek reaches and the Cedar Creek and Golden Ridge Creek tributaries. Statistics of residence time, T_r, and sediment age, T_a, distributions include mean, $\overline{T}$, standard deviation, σ_T, median, T_{50}, and 90th percentile, T_{90}; 95% confidence limits (in square brackets) represent uncertainty due to sampling error in determination of inherited age distributions used in correcting residence times (see text); uncorrected values in parentheses; all times are calibrated years. For flux calculation, deposit bulk density = 1.26×10^3 kg/m^3 (Lancaster et al., 2010). For efficiency calculation, weathered bedrock density = 2.27×10^3 kg/m^3 (Anderson et al., 2002); bedrock lowering rate = 1.17×10^{-4} m/yr (Heimsath et al., 2001); so unit mass flux = 0.266 kg/m^2/yr in upstream contributing area.
[b] Number in parentheses is local contributing area (total area minus upper basin area).
[c] Estimate for lower Bear Creek uses (8), whereas others use (7).

the uppermost tips of the valley network (Wells and Peck, 1961). Tree roots and understory vegetation stabilize soils, slow bioturbation dominates soil transport, and occasional landslides are associated with tree mortality (e.g., from drought and pestilence). Fires remove understory vegetation, kill the trees and their roots, and thereby lead to brief periods ($\lesssim$ 10 weeks) of rapid hillslope transport via dry ravel, which may account for 40%–80% of all transport on the steepest slopes (Roering and Gerber, 2005), and longer periods ($\sim$ 10–50 yr) of rain-induced landsliding via mass failure of colluvium in hillslope hollows (i.e., unchanneled convergent areas) and transport via debris flow to the downstream valley network. While overland-flow erosion upstream of channel heads is limited to expansion of bedrock areas already exposed by mass movement, high flows in steep channels can, in the absence of dams formed by fallen trees and woody debris-flow deposits, typically transport all supplied sediment (Benda and Dunne, 1997a; Dietrich and Dunne, 1978; Jackson and Roering, 2009; Lancaster et al., 2001; Lancaster and Grant, 2006; May, 2002; May and Gresswell, 2003; Montgomery et al., 2000; Reneau and Dietrich, 1991; Roering et al., 2003; Schmidt et al., 2001; Swanson, 1981).

However, in the presence of such dams, concomitant deposits appear to have unusually high charcoal concentrations relative to other environments in the western USA. On headwater valley floors in the Oregon Coast Range, a few shovelfuls of sediment from a small ($\sim$ 15 cm $\times$15 cm) area within any unit typically yields sufficient charcoal for multiple radiocarbon dates (e.g., Frueh, 2011, dated 258 charcoal samples from 134 randomly selected units). In contrast, sampling in the Rocky Mountains usually requires searching for charcoal-rich units (Grant A. Meyer, personal communication, 2013). So old wood, slow bioturbation, lengthy storage in hollows, and reworking of valley-floor deposits are sufficient to create inherited ages of $\sim 10^2$ to 10^4 yr in the Oregon Coast Range, but young exterior wood and the extraordinary rapidity and dominance of post-fire sediment transport may compress charcoal histories sufficiently for negligible inherited ages in most, if not all, cases (Lancaster and Casebeer, 2007; Lancaster et al., 2010; May and Gresswell, 2003; Reneau and Dietrich, 1991; Sweeney et al., 2012).

We collected samples and other data from debris-flow and fluvial deposits on the headwater valley floor of Knowles Creek, a tributary to the Siuslaw River in the Oregon Coast Range (Fig. 1). Mainstem stream gradients range from 1.4 to 17% and contributing areas from 0.3 to 5.0 km^2. Sampling sites have lithology, vegetation, climate, and depositional settings similar to those of nearby sites: Bear Creek, tributary to Knowles Creek (Lancaster and Casebeer, 2007); Cedar Creek, in the Siuslaw River basin; and Golden Ridge Creek, in the North Fork Smith River basin (Lancaster et al., 2010). The Bear Creek site comprises deposits on two adjacent reaches of the valley floor. The Cedar Creek site comprises a debris-flow fan at the mouth of a small tributary, where the fan is incised by two channels, plus the deposits on the adjacent mainstem, 120 m in length. The Golden Ridge Creek site comprises predominantly fluvial deposits at a tributary mouth, where the deposits are incised by a braided channel, plus the deposits on the adjacent mainstem, 57 m in length (Table 1).

The study areas are almost entirely forested by large conifers, even in riparian zones (Ohmann and Gregory, 2002). From such riparian conditions, we infer that recent disturbances, whether anthropogenic (road building, timber harvest) or natural (fire, pestilence), have had no detectable effect, with the exceptions of two debris-flow runout tracks in upper Bear Creek, one that may be associated with timber harvest and another associated with a large storm ca 1996 and originating in mature forest, and a long-abandoned narrow roadbed along Cedar Creek, presumably where logs were dragged to a log drive on nearby Sweet Creek (Miller, 2010).

3. Methods

3.1. Sample Ages

In addition to the sites of Lancaster and Casebeer (2007) and Lancaster et al. (2010), we chose 14 new sample sites in Knowles Creek from a larger set of randomly selected sites, with selection probability weighted by sediment volume and bank area (Fig. 1, Table A.1 in supplement). The new sites represent the different facies sampled by Lancaster and Casebeer (2007) and Lancaster et al. (2010) and, by comprising a range of contributing watershed areas, different potentials for upstream charcoal storage (Table 2). We recorded bank stratigraphy over the accessible column at each sample site and classified the facies for each stratum as debris-flow

deposit (poorly sorted silt- to boulder-sized particles with matrix-supported clasts), fluvial fines (stratified sand and finer particles), or fluvial gravels (rounded, imbricated, clast-supported gravel and interstitial sand) (Costa, 1984). Stratigraphic units were differentiated according to facies type, texture, color, and induration (Fig. 2).

The location of each sampling site was specified by a distance along the mainstem or tributary channel and a depth below the top of the bank. Despite the wide ranges in texture observed for both fluvial gravels and debris-flow deposits, boundaries between units may be obscure, and fluvial fines often form thin strata that are typically lumped into a single unit. Therefore, all samples were taken from the same stratigraphic unit and within ±7.5 cm in the vertical direction and ±15 cm (±7.5 cm for all but a few sites) in the streamwise direction. Units thinner than ~ 15 cm were excluded, as were one or two units that yielded insufficient charcoal.

We sampled charcoal because it is more resistant to decomposition than uncharred wood and provides consistency for analysis. We avoided disturbed sediment (e.g., animal burrows, root wads) to reduce the potential for sampling material emplaced after deposition, although bioturbated sediment is not always recognizable, especially in debris-flow deposits and unstratified fluvial gravels. We gently sifted sediment to reduce breakage of charcoal pieces and discarded those recently broken (e.g., with shiny surfaces) to eliminate redundant dating.

According to standard protocol, multiple charcoal samples (N = 6–13) were taken from the stratum, or depositional unit, located at each sampling site, pretreated with acid–base–acid washes to remove fulvic and humic acids, combusted to CO_2 in sealed 6-mm-diameter glass tubes, and sent to the University of Arizona for radiocarbon dating via AMS. At least ten samples per unit were taken, but some were too small for AMS dating after pretreatment. At 4 locations (2611-L, 2778-R, 3770-R, and 4194-R) we found fewer than 10 sufficiently large pieces and, instead, substituted collections, or composites, of smaller pieces for 7 of 127 samples. Radiocarbon age calibration for both the new Knowles Creek samples and those of Lancaster and Casebeer (2007) and Lancaster et al. (2010) employed the IntCal09 and Bomb04NH1 calibration curves (Reimer et al., 2009; Hua and Barbetti, 2004).

Table 2
Sampling sites, minimum sample ages, and inherited age statistics[a].

Unit	Ht. (m)	Type	CA (km^2)	Min. age (a BP)	Inherited age (yr)				Min./ Total
					$\bar{I}$	σ_I	I_{50}	I_{90}	
2778-R	1.7	DF	0.08	981	1264	2181	300	6840	2/9
3397-Ra	1.4	DF	0.05	174	614	669	325	1880	1/10
3397-Rb	1.1	DF	0.05	411	88	133	70	275	6/9
4048-R	0.6	DF	< 0.01	1449	1677	3688	40	9870	5/6
4204-RT-R	0.4	DF	0.09	140	1067	1066	990	3640	2/10
4254-RT-R	0.5	DF	0.16	137	61	165	40	275	8/9
4414-RT-R	0.8	DF	0.42	165	299	203	320	535	2/10
3770-R	1.0	FF	3.29	5097	1038	1219	280	2740	4/8
4194-R	1.3	FF	4.16	7530	629	621	465	1730	2/10
4534-L	1.0	FF	4.91	470	488	629	205	1400	3/11
2013-La	0.9	FG	1.09	152	1184	2045	350	5840	5/13
2013-Lb	0.3	FG	1.09	166	2698	2803	1280	8120	2/8
2611-L	0.2	FG	1.76	800	609	780	200	2010	3/8
4379-L	0.3	FG	4.44	439	1810	1996	1030	5770	1/6

[a] Sampling sites identified by unit number (Unit), indicating distance (m) downstream from divide, right (R) or left (L) channel bank, facing downstream, or right bank of right-bank tributary (RTR); height (m) above low-flow water surface or dry thalweg (Ht.); deposit type, or facies (Type), whether debris-flow deposit (DF), fluvial fines (FF), or fluvial gravels (FG) (Fig. 1); and upstream contributing area (CA). Minimum sample age for the unit (Min. age) given in calibrated years before AD 1950 (a BP). Inherited age statistics comprise mean, $\bar{I}$, standard deviation, σ_I, median, I_{50}, and 90th percentile, I_{90}, of the inherited age PDF for each unit from equation (2) in calibrated years (yr); and number of samples with mean calibrated ages, $\overline{A_j}$, within 95% confidence limits of minimum mean age, $\overline{A_{min}}$, including minimum-age sample, vs. total number of samples.

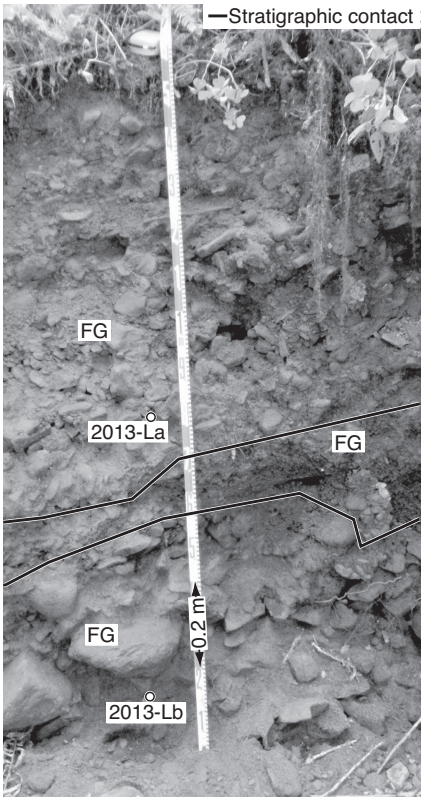

Fig. 2. Interpreted stratigraphic section (FG = fluvial gravel) at location of samples 2013-La and 2013-Lb (small white circles; Fig. 1, Table 2). Top and bottom depositional units are separated by a thin fluvial gravel unit with intermediate diameters < 2 cm. Bottom of measuring tape is 0.2 m above thalweg, from which sample heights were measured (Table 2).

Lancaster and Casebeer (2007) and Lancaster et al. (2010) also weighted probabilities of sampling random stream-bank and terrace-riser locations by deposit volume and bank or riser area. Lancaster and Casebeer (2007) sampled 60 sites (30 in each of the two valley reaches) along Bear Creek, radiocarbon dated 44 samples, inferred ten ages by stratigraphic correlation with dated sites, and inferred six from known provenance (a large storm in 1996) of a large debris-flow deposit (Fig. 1; Tables A.2, A.3 in supplement). Lancaster et al. (2010) sampled 30 sites along the channels incising the fan on Cedar Creek, five sites along the adjacent mainstem, 24 sites along the Golden Ridge Creek tributary, and 8 sites along the mainstem; they radiocarbon dated all 67 samples (Fig. 1; Tables A.4, A.5 in supplement).

3.2. Inherited Ages

Whereas the inherited age is the difference between the calibrated sample age and the actual deposit age, where the latter is assumed equal to the minimum calibrated age of samples from the same unit, and these ages are all random variables, the inherited age distribution of the j^{th} sample is the convolution of the sample and deposit age probability distributions:

$$F_{I_j}(t) = \int_{-\infty}^{\infty} F_{A_j}(t + t')\, f_{A_{min}}(t')\, \mathrm{d}t', \qquad (1)$$

where F and f denote the cumulative distribution function (CDF) and PDF, respectively, of the random variable in the subscript; t is the value of the random variable; I_j, A_j, and A_{min} are the random

variables representing inherited age for charcoal sample j, calibrated age of sample j, and minimum calibrated age of samples from the same unit, respectively; and t' is a dummy variable of integration.

To find the distribution of inherited ages for a given unit, or all units of a given facies (i.e., debris-flow deposits, fluvial fines, fluvial gravels), PDFs of individual inherited ages were summed and renormalized:

$$f_I(t) = \frac{1}{N_u} \sum_{j=1}^{N_u} f_{I_j}(t) \tag{2}$$

where I is the random variable representing inherited age for a set of N_u samples from the same unit, a set that includes the convolution of the minimum age PDF with itself, and $f_{I_j}(t) = \mathrm{d}F_{I_j}(t)/\mathrm{d}t$. According to (1) and (2), probability of negative inherited age can, in general, be non-zero, reflecting the uncertainty in minimum age.

Although negative errors are possible, e.g., due to bioturbation, inherited ages are non-negative by definition, so PDFs including all units of each facies (debris-flow deposits, fluvial fines, and fluvial gravels) in Knowles Creek are restricted to non-negative inherited ages. Equation (2) therefore becomes

$$f_{I_f}(t) = \frac{\sum_{j=1}^{N_f} f_{I_j|I_j\geq 0}(t \mid t \geq 0)}{\sum_{j=1}^{N_f} \left[\int_0^\infty f_{I_j}(t')\,\mathrm{d}t' \right]}, \tag{3}$$

where random variable I_f represents non-negative inherited age for a set of N_f samples of a single deposit type, or facies. The foregoing age corrections use smooth PDFs to represent the underlying distributions of inherited age for each facies, and the Weibull distribution, among common distribution functions (including gamma, exponential, and generalized Pareto), provided the best fit to observed inherited age distributions. We estimated the parameters of the Weibull PDF,

$$f_{I_f}(t) = \begin{cases} \frac{b_W}{a_W} \left(\frac{t}{a_W}\right)^{b_W - 1} e^{-(t/a_W)^{b_W}}, & t > 0 \\ 0, & t \leq 0, \end{cases} \tag{4}$$

with scale parameter, a_W (yr), and shape parameter, b_W, by nonlinear least-squares curve fitting of the Weibull CDF to the observed, log-transformed CDF. This method reduces the influence of small probabilities in the greater-age tails. We restricted each fit to $F_{I_f}(t) < 0.99$ in order to eliminate a disproportionate influence of the tail of the oldest sample.

3.3. Deposit Ages

Conceptually, corrected deposit age, T'_d, is the difference between the apparent, or uncorrected, deposit age, T_d, which is equivalent to the sample age, and the inherited age, I_f. However, because these are random variables, this "difference" is calculated via convolution, or

$$F_{T'_d}(t) = \begin{cases} \dfrac{\int_{-\infty}^{\infty} \left[F_{T_d}(t+t') - F_{T_d}(t')\right] f_{I_f}(t')\,\mathrm{d}t'}{\int_{-\infty}^{\infty} \left[1 - F_{T_d}(t')\right] f_{I_f}(t')\,\mathrm{d}t'}, & t \geq 0 \\ 0, & t < 0, \end{cases} \tag{5}$$

which is conditional on non-negative corrected deposit ages, and the PDF is $f_{T'_d}(t) = \mathrm{d}F_{T'_d}(t)/\mathrm{d}t$. We assume that facies-specific inherited age distributions for charcoal in Knowles Creek are the same for charcoal and other woody material dated by Lancaster and Casebeer (2007) and (Lancaster et al., 2010) in similar sites (Tables A.3–A.5 in supplement), because we do not have inherited age data specific to uncharred woody material.

Fifty-four of sixty deposit ages from Bear Creek and all ages from the Cedar Creek and Golden Ridge Creek sites were corrected with equation (5). Six deposit ages were inferred from the known age of a recent debris flow in upper Bear Creek (Lancaster and Casebeer, 2007) and were not corrected (Table A.3 in supplement).

The residence time distributions, both corrected with equation (5) and not, as inferred from deposit ages found along the two Bear Creek reaches and the Cedar Creek and Golden Ridge Creek tributaries, are nevertheless corrected for age inversions: where deposit ages suggest that older deposits overlie younger, and the 95% confidence interval of either distribution (apparent or corrected) excludes the mean of the other, the lower age distribution is substituted for the upper.

3.4. Sediment Ages and Residence Times

Reservoir mass flux, Q_R, or time-averaged sediment flux passing through a valley-floor reservoir, is (Eriksson, 1971):

$$Q_R = \frac{M_0}{\overline{T_r}} \tag{6}$$

where the mass of material in the reservoir is $M_0 = V_0\rho_b$; $\overline{T_r}$ is the mean residence time; V_0 is valley-floor sediment volume, calculated from field surveys (Lancaster and Casebeer, 2007; Lancaster et al., 2010); and bulk density of sediment is $\rho_b = 1.26 \times 10^3$ kg/m^3 (Lancaster et al., 2010). Trapping efficiency, E_t, is the fraction of basin sediment yield contributing to reservoir mass flux. Assuming that all watershed areas contribute equally to storage,

$$E_t = \frac{Q_R}{A_{ds}\varepsilon\rho_r}, \tag{7}$$

where A_{ds} is the contributing area at the downstream end of the reach; bedrock lowering rate is $\varepsilon = 1.17 \times 10^{-4}$ m/yr (Heimsath et al., 2001); and bedrock density is $\rho_r = 2.27 \times 10^3$ kg/m^3 (Anderson et al., 2002). For lower Bear Creek, which has a substantial percentage of debris-flow deposits that all originate in local tributaries, we assume that only local areas contribute to debris-flow deposits in proportion to their respective fraction among sampling sites:

$$E_t = \frac{Q_R}{A_{ds}\varepsilon\rho_r}\left(1 + \frac{p_d A_{us}}{A_{ds} - A_{us}}\right) \tag{8}$$

where A_{us} is the contributing area at the upstream end of the reach; and p_d is the fraction of charcoal samples taken from debris-flow deposits. These assumptions imply that local areas, which comprise 39.5% of the total basin area, contribute 59.4% of the reservoir mass flux of lower Bear Creek.

Stream banks, and some terrace risers, are the surfaces from which sediment is eroded and thereby leaves the reservoir comprising valley-floor deposits. We therefore infer that ages of deposits exposed in these surfaces are representative of, and equivalent to, residence times. We assume that the distribution of these residence times, sampled over space at an instant in time, is representative of the steady-state distribution (Lancaster and Casebeer, 2007; Lancaster et al., 2010). The residence time distribution, then, is the

normalized sum of the individual deposit age distributions:

$$F_{T_r}(t) = \frac{1}{N_d}\sum_{i=1}^{N_d} F_{T_{di}}(t), \tag{9}$$

where the random variable, T_r, represents residence times in the reservoir; N_d is the number of deposit ages included in the distribution; the random variable T_{di} represents the i^{th} deposit age; and the individual deposit age distributions, $F_{T_{di}}(t)$, can be uncorrected or corrected with (5).

According to Bolin and Rodhe (1973) and (6), the sediment age PDF and residence time CDF are related by

$$f_{T_a}(t) = \frac{1}{\overline{T_r}}\left[1 - F_{T_r}(t)\right], \tag{10}$$

where the random variable, T_a, represents sediment ages in the reservoir, and the quantity within the square brackets is typically called the exceedance distribution, survival function, or tail function. The probability of evacuation is then given by the hazard rate function [1/T] (Sigman, 1999),

$$h_{T_a}(t) = \frac{f_{T_r}(t)}{\overline{T_r} f_{T_a}(t)}. \tag{11}$$

For exponentially distributed residence times, the sediment age and residence time distributions (and their means) are equivalent, and evacuation probability is constant with respect to sediment age. For distributions that decay more slowly than an exponential (i.e., with thicker tails), such as the gamma and Weibull distributions with shape factors less than one, and the Pareto (power-law) distribution, mean sediment age is greater than mean residence time, and evacuation probability declines monotonically with age (Bolin and Rodhe, 1973; Dietrich et al., 1982; Lancaster and Casebeer, 2007; Lancaster et al., 2010; Makhnin, 2010; Sigman, 1999). We fit the gamma CDF,

$$F_{T_r}(t) = \begin{cases} \dfrac{1}{b_\Gamma^{a_\Gamma}\Gamma(a_\Gamma)}\displaystyle\int_0^t t'^{a_\Gamma - 1} e^{-t'/b_\Gamma}\,\mathrm{d}t', & t > 0 \\ 0, & t \le 0 \end{cases} \tag{12}$$

to the residence time distributions from (9) with the method of moments, wherein the shape parameter is $a_\Gamma = \overline{T_r}^2/\sigma_{T_r}^2$, and the scale parameter is $b_\Gamma = \sigma_{T_r}^2/\overline{T_r}$ (yr), where σ_{T_r} is the residence time standard deviation, and we used nonlinear least-squares curve-fitting to fit exponential and power-law distributions.

3.5. Uncertainty Due to Sampling Error

"Sampling error" at the Knowles Creek sites might result in differences between true deposit ages and minimum charcoal sample ages, and the potential for such error produces uncertainties in inherited and corrected deposit ages and residence times. We constrained these uncertainties through bootstrapping (Efron and Tibshirani, 1993). From the original sets of N_u samples from each Knowles Creek depositional unit, we randomly resampled, with replacement, new sets of N_u samples from each unit and recalculated inherited ages and Weibull fits to the facies-specific distributions. We repeated this process 10,000 times. We then recalculated, 10,000 times, age corrections based on Weibull parameters randomly selected from the bootstrapped estimates. For all quantities calculated from the Knowles Creek sample ages, we inferred 95% confidence limits from the 2.5th and 97.5th percentiles of the bootstrapped estimates of those quantities. These confidence limits therefore represent the propagation of uncertainty arising from sampling at each Knowles Creek site to determine inherited ages but do not represent, for example, any uncertainty arising from the selection of either the inherited-age or residence-time sampling sites.

4. Results

4.1. Knowles Creek Sample Ages

Minimum mean calibrated ages of Knowles Creek samples range from 143 to 7530 a BP (Fig. 1; Table A.1 in supplement), and the percentage of mean calibrated ages that are within two standard deviations of the minimum in each unit ranges from 0% to 88%, excluding the minimum mean ages themselves (Table 2).

4.2. Inherited Ages

For the inherited age PDFs calculated from (2) for each unit (Fig. 3, Table 2), mean inherited ages for the units, $\overline{I}$, span more than an order of magnitude, from 61 to 2700 yr, and are uncorrelated with the minimum mean sample ages or contributing watershed areas (e.g., F statistic p-value = 0.4 for exponential regression), and similarly for standard deviation, σ_I.

Distributions of inherited age for each facies, or deposit type, from (3) show that the distribution mean, $\overline{I_f}$, median, I_{f50}, and 90th percentile, I_{f90}, are greatest for fluvial gravels and smallest for debris-flow deposits, and the exceedance distribution for fluvial gravels decays more slowly than the others between 200 and 2000 yr (Table 3, Fig. 4). The overall shape of the inherited age exceedance distribution for debris-flow deposits is steeper than for fluvial fines, but the distribution tail for debris-flow deposits extends to greater ages than for either fluvial fines or fluvial gravels: 99th percentiles of inherited ages are 9890, 2940, and 8250 yr for debris-flow deposits, fluvial fines, and fluvial gravels, respectively. This long tail for debris-flow deposits influences both the mean and standard deviation to the extent that the means for debris-flow deposits and fluvial fines are similar, and the standard deviation is greater for debris-flow deposits. Sampling error at the individual units introduces uncertainties to the estimates of the facies-specific mean inherited ages of approximately ±50%, so that only the mean inherited age for fluvial gravel is significantly different from the other two.

Weibull distributions fit to the facies-specific inherited age CDFs have scale parameters less than, but similar to, the means ($a_W \lesssim \overline{I_f}$)

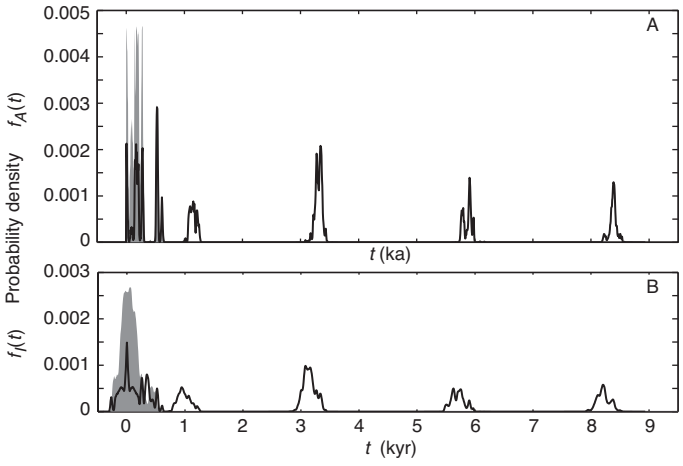

Fig. 3. Normalized probability density functions of calibrated sample ages, $f_A(t)$ (A), and inherited ages $f_I(t)$ (B) at sites 2013-Lb (black line) and 4254-RTR (gray fill), sites with the largest and smallest mean inherited ages, respectively (Table 2).

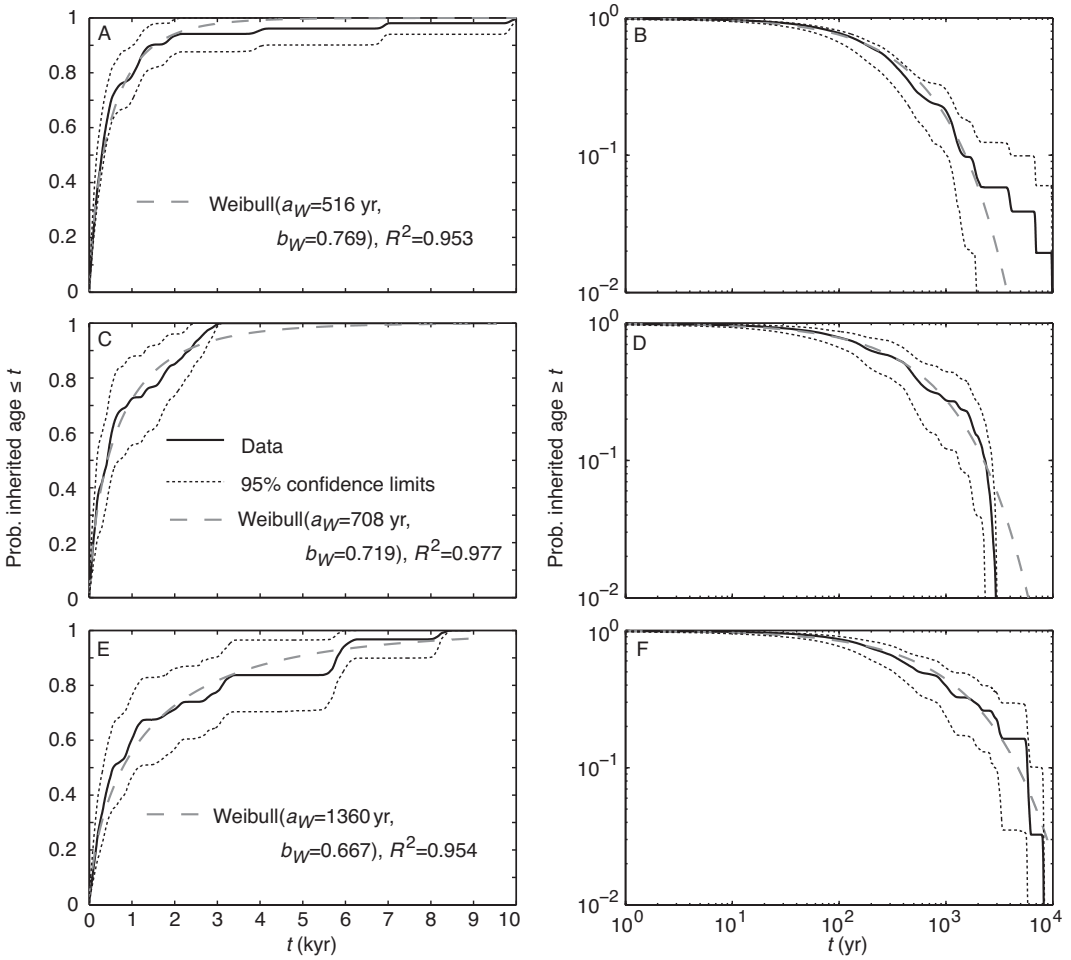

Fig. 4. Cumulative (A,C,E) and exceedance (B,D,F) distribution functions of inherited age, $F_{I_f}(t)$ and $1 - F_{I_f}(t)$, respectively, from data (black lines), where $F_{I_f}(t)$ is the integral of (3), with 95% confidence limits (thin dotted black lines), and fitted Weibull distributions, the integral of (4) (gray dashed lines)(1 kyr = 1000 yr) for debris-flow deposits (A,B), fluvial fines (C,D), and fluvial gravels (E,F). Fractions of variance explained, R^2, shown for fits to CDFs. Confidence intervals are properly interpreted as intervals of inherited age (x-axis) rather than intervals of probability (y-axis).

and shape factors less than one ($b_W < 1$), so the distributions are heavy-tailed (Sigman, 1999). The fits all have $R^2 > 0.95$ and predict inherited ages within the bootstrapped 95% confidence limits for $F_{I_f}(t) \leq 0.99996$, 0.93, and 0.96 for debris-flow deposits, fluvial fines, and fluvial gravels, respectively (Table 3, Fig. 4). Typical of heavy-tailed distributions, standard deviations are greater than means, means are two to three times greater than medians, and the 90th percentiles, all greater than 1000 yr, are roughly an order of magnitude greater than the medians, all less than 500 yr (Table 3). Given the 95% confidence limits for the fitted values of the shape parameter, b_W, the differences among the values for the three facies, debris-flow deposits, fluvial fines, and fluvial gravels, may not be significant (Table 3). For the scale parameter, a_W, the difference between the fitted values for debris-flow deposits and fluvial fines may not be significant, but the value for fluvial gravels is greater than for the other two facies, and according to the bootstrapped confidence limits, the difference is apparently significant (Table 3).

Table 3
Inherited age statistics for deposit types[a].

	Debris-flow	Fluvial fines	Fluvial gravels
N	62	29	35
$\overline{I_f}$	817 [418, 1280]	780 [472, 1080]	1730 [1030, 2440]
σ_{I_f}	1690 [482, 2500]	868 [594, 1020]	2230 [1430, 2770]
I_{f50}	295 [175, 360]	425 [180, 705]	565 [325, 1150]
I_{f90}	1450 [1020, 4100]	2340 [1310, 7100]	5800 [2890, 7860]
a_W	516 [336, 724]	708 [387, 1200]	1360 [755, 2270]
b_W	0.769 [0.595, 0.833]	0.719 [0.570, 0.857]	0.667 [0.506, 0.786]

[a] Summary of inherited ages in calibrated years (yr) for each deposit type, where N is the number of samples from each deposit type; $\overline{I_f}$, σ_{I_f}, I_{f50}, and I_{f90}, are mean, standard deviation, median, and 90th percentile, respectively, of non-negative inherited age PDFs (3); a_W and b_W are scale (yr) and shape parameters for the Weibull distribution (4); and 95% confidence limits (in square brackets) represent uncertainty due to sampling error in determination of inherited age distributions used in correcting residence times (see text).

4.3. Corrected Deposit Ages and Residence Times

Corrected deposit age PDFs are smoother, wider, and shifted toward younger ages, but the forced truncation at zero age in (5) produced less widening and smaller absolute reductions for younger samples, although relative changes were generally smallest for the oldest samples (Fig. 5). Distribution means decreased by 29%, on average (Fig. 5; Tables A.3–A.5 in supplement). Correction reduced post-bomb (after AD 1950) age estimates by 20%–44% for the youngest to oldest samples, respectively. For pre-bomb ages, the youngest age estimates were reduced by 31%–36%, the oldest by 14%–22%. In the case of the oldest (BC-26) and youngest (BC-27) samples from lower Bear Creek, for example, corrected mean deposit ages are 22% (3990 vs. 5120 yr) and 32% (123 vs. 181 yr), respectively, less than uncorrected, and corrected stan-

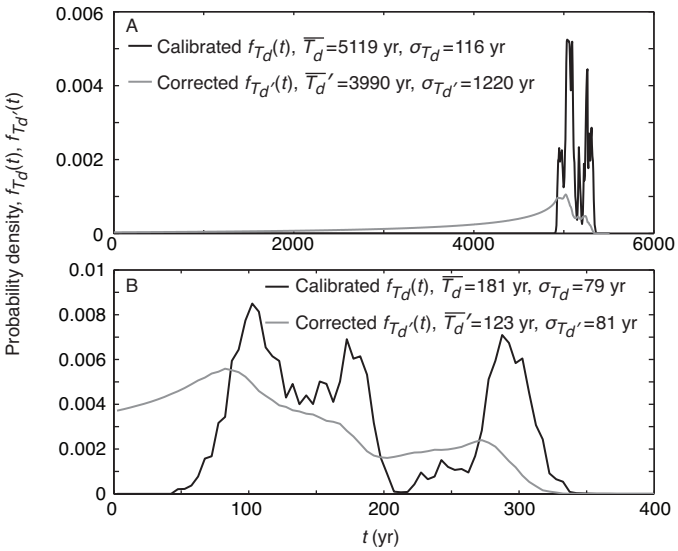

Fig. 5. Uncorrected (calibrated) and corrected probability density functions of deposit ages for samples BC-26 (A) and BC-27 (B), lower Bear Creek's oldest and youngest samples, respectively (Table A.2 in supplement) (Lancaster and Casebeer, 2007), with deposit age means, $\overline{T_d}$ and $\overline{T_d'}$, and standard deviations, σ_{T_d} and $\sigma_{T_d'}$, all in calibrated years relative to time of sampling, AD 2003. Correction is by convolution with the Weibull fit of Fig. 4E.

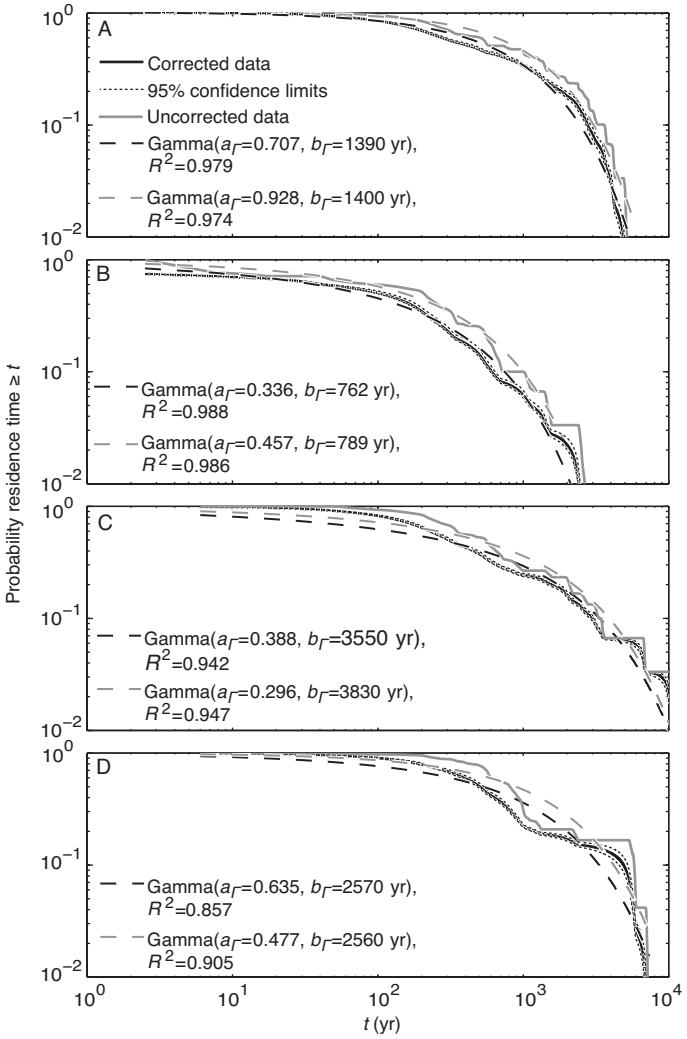

Fig. 6. Residence time exceedance distributions, $1 - F_{T_r}(t)$, inferred from bank-deposit ages, both "corrected" with equation (5) and not ("uncorrected"), and all corrected for age inversions, for lower (A) and upper (B) Bear Creek and the Cedar Creek (C) and Golden Ridge Creek (D) tributaries. Confidence limits for corrected distributions indicate bootstrapped uncertainty from potential sampling error in determination of inherited ages. Gamma distributions fit to corrected (dashed black) and uncorrected (dashed gray) distributions by the method of moments, with shape and scale parameters, a_Γ and b_Γ, respectively, and fractions of variance explained by the fits, R^2. Confidence intervals are properly interpreted as intervals of time, t (x-axis), rather than intervals of probability (y-axis).

dard deviations are 950% (1220 vs. 116 yr) and 2.8% (81 vs. 79 yr), respectively, greater than uncorrected (Fig. 5, Table A.2 in supplement).

Residence time distributions for the four valley-floor sediment reservoirs comprising the deposits at each site, upper and lower Bear Creek and the Cedar and Golden Ridge Creek tributaries, were calculated from (9), and sediment age PDFs were calculated from (10). (Due to the small numbers of samples from mainstem Cedar and Golden Ridge Creeks, these samples were not included in the analyses.) Correction for inherited age smoothed the distributions and shifted them towards shorter times, shifts that effectively narrowed the residence time distributions, so that means ($\overline{T_r}$), medians (T_{r50}), 90th percentiles (T_{r90}), and standard deviations (σ_{T_r}) were all smaller after inherited age correction (Table 1). For the same storage volume, shorter mean residence times imply greater fluxes and, therefore, trapping efficiencies, as calculated with (6), (7), and (8) (Table 1). Relative changes in mean residence time were greater than for standard deviation at all four sites: correction reduced estimates of the mean by 24.7%, 29.1%, 16.8%, and 25.2% for lower and upper Bear Creek reaches and the Cedar and Golden Ridge Creek tributaries, respectively, or 24.0% on average across sites, and standard deviations by 13.4%, 17.1%, 5.43%, and 14.2%, respectively, or 12.5% on average (Table 1). Sediment ages decreased less than did residence times or, in the case of the Cedar Creek fan, increased slightly due to correction, so the inferred differences between sediment ages and residence times increased (Table 1).

Consistent with the above results, residence time distributions had thicker tails after correction, in that gamma shape parameters were smaller, and exponential distributions were poorer fits (smaller R^2; Fig. 6, Table 4). The changes in gamma shape parameters are significant in the sense that none of the confidence limits of the corrected values includes the uncorrected estimate. Changes in the exponents of power-law fits provide ambiguous and inconsistent results, but essential implications are similar before and after correction: the third and higher moments are undefined for lower Bear Creek; the second and higher moments are undefined for upper Bear; and the first and higher moments are undefined for the Cedar and Golden Ridge Creek tributary deposits (Sigman, 1999) (Table 4).

Of 19 locations with clear stratigraphic relationships in lower and upper Bear Creek, the Cedar Creek tributary and mainstem, and the Golden Ridge Creek tributary and mainstem, there were 3 age inversions. Differences between corrected mean deposit ages of the upper and lower samples were 400, 3410, and 778 yr for age inversions in lower and upper Bear Creek and the Golden Ridge Creek tributary, respectively (Tables A.2–A.5 in supplement).

Perhaps surprisingly, the relatively large uncertainties in inherited ages due to sampling error do not produce large uncertainties in the corrected residence time distributions. For example, none of the mean residence times, standard deviations, medians, or 90th percentiles falls within the relevant confidence intervals for any of the other sites, and similarly, the parameters of the gamma distributions fit to the residence time distributions by the method of moments are each significantly different from the rest.

Table 4
Parameters of fits to residence time distributions[a].

		Lower Bear	Upper Bear	Cedar fan	Golden Ridge trib.
Uncorrected					
Gamma:	a_Γ	0.928	0.457	0.388	0.635
	b_Γ (yr)	1400	789	3550	2570
	R^2 (%)	97.4	98.6	94.2	85.7
Power:	α	2.17 ± 0.05	1.14 ± 0.02	0.775 ± 0.006	0.734 ± 0.010
	R^2 (%)	94.8	97.5	96.3	91.5
Exponential:	μ (yr)	1310 ± 10	313 ± 8	1040 ± 10	1370 ± 30
	R^2 (%)	96.5	91.0	88.5	81.7
Corrected					
Gamma:	a_Γ	0.707 [0.692, 0.738]	0.336 [0.330, 0.357]	0.296 [0.291, 0.308]	0.477 [0.463, 0.496]
	b_Γ (yr)	1390 [1340, 1430]	762 [738, 791]	3830 [3730, 3870]	2560 [2440, 2680]
	R^2 (%)	97.9	98.8	94.7	90.5
Power:	α	2.50 ± 0.04	1.16 ± 0.01	0.736 ± 0.006	0.745 ± 0.009
	R^2 (%)	96.8	99.2	96.4	94.8
Exponential:	μ (yr)	944 ± 16	201 ± 7	750 ± 15	923 ± 22
	R^2 (%)	92.2	84.8	79.3	80.5

[a] Parameters of fits to residence time exceedance distributions, $P = 1 - F_{T_r}(t)$, with fractions of variance explained, R^2 (Fig. 6), for upper and lower reaches of Bear Creek, the debris-flow fan of a tributary to Cedar Creek, and the valley-floor deposits in the mouth of a tributary to Golden Ridge Creek. Gamma distribution (12): a_Γ is shape parameter, b_Γ (yr) is scale parameter, fit by method of moments; 95% confidence limits (in square brackets) represent uncertainty due to sampling error in determination of inherited age distributions used in correcting residence times (see text). Power-law: α (± confidence limits from root mean square error) is exponent in $P = \beta t^{-\alpha}$, for $t > 2000$ yr for lower Bear Creek, and $t > 200$ yr for upper Bear, Cedar fan, and Golden Ridge tributary, fit by nonlinear least squares. Exponential: μ (± 95% confidence limits from root mean square error) is scale parameter of exponential distribution, $P = \exp(-t/\mu)$, fit by nonlinear least squares.

5. Discussion

5.1. Uncertainty

Accurate estimation of inherited age depends on accurate estimation of true deposit age, but unless deposit age is known *a priori*, that "true" deposit age is itself a random variable. Moreover, eliminating that random variable, say, by sampling only deposits of known age (e.g., via air-photo and field surveys) would violate our protocol of random sampling and add an unknown, unquantifiable bias to our inherited age estimates. Limiting sampling to deposits $\lesssim$ 100 yr old would also likely lead to larger calibration uncertainties. As bootstrapping provides robust estimation of the uncertainty introduced by the estimation of true deposit age, we have opted in favor of unbiased estimation of inherited age with quantifiable uncertainty at the cost, perhaps, of some accuracy, as is standard practice in choosing estimators for random variables (e.g., Benjamin and Cornell, 1970). And bootstrapping reveals substantial uncertainties for inherited ages: for the facies-specific inherited age distributions, 95% confidence intervals are approximately ±40% to 50% for the means, ±35% to 70% for the best-fit Weibull scale parameters, a_W, and ±10% to 25% for the shape parameters, b_W (Fig. 5). However, the resulting uncertainties in corrected deposit ages and residence times are relatively small, both $\sim$ ±1% to 10%.

5.2. Inherited Age

Right-skewed inherited age distributions peaked at zero age imply that charcoal entering all sampled deposits at our sites is predominantly young at the time of deposition, and we reason that these young-age peaks reflect high rates of sediment transport following fire. The long tails of those distributions imply some entrainment and deposition of old charcoal with ages spanning thousands of years. Mechanisms contributing to these long tails might include long but finite lifespans of trees (i.e., inbuilt ages) and episodic evacuation of sediment from upslope storage, especially in the unchanneled extremities of the valley network. Differences among the facies-specific distributions may reflect differences among, primarily, conditions promoting deposition of these facies and, secondarily, the charcoal and sediment reservoirs tapped by fluvial and debris-flow transport. Although the observed inherited age distributions reflect conditions specific to the geomorphology and forest environment of the Oregon Coast Range, similar processes and mechanisms are active elsewhere, albeit with effects of different magnitudes. Moreover, sampling protocol may have the largest effect on both inherited age means and distribution shapes. Given our sampling sites and protocol and the range of observed inherited ages, we reason that inherited age magnitudes and distribution shapes predominantly reflect upslope storage and a relatively small contribution by inbuilt ages.

5.2.1. Common Controls

Both inbuilt ages and residence times in prior storage may contribute to inherited ages. The interaction of fire and fuel creates an "original" inbuilt age distribution, i.e., for all the charcoal produced in the fire. Growth, mortality, and decay rates determine quantities and age distributions of flammable surfaces. Surface area, material properties, and external factors determine fire size and intensity and, therefore, the relative rates of flaming combustion, which consumes the volatilized fraction, and glowing combustion, which consumes the charred fraction. Charring itself provides energy for volatilization but also insulates interior wood from further combustion (Friquin, 2011; Lowden and Hull, 2013; Sullivan and Ball, 2012).

The live biomass consumed or charred by even the most severe fires predominantly comprises the youngest material, such as needles, cones, seeds, bark, ground litter, and finer branches of the canopy and understory, and selection of these materials can minimize or effectively eliminate inbuilt ages (Scott, 2010). High-intensity fires, such as those typical of the coastal ranges of the Pacific Northwest, may incinerate finer organic material in the canopy and near the soil surface and leave only charcoal from charred wood. For example, charring at a typical rate of 0.6 mm s^{-1} over the woody surface area of a 400-yr-old Douglas-fir in the Pacific Northwest would produce energy sufficient to volatilize all of the needles in 0.3 s (Friquin, 2011; Lowden and Hull, 2013; Pike et al., 1977; Sullivan et al., 2003; Sullivan and Ball, 2012).

Only dead biomass, i.e., standing snags and fallen logs, is deeply charred by fire, but even for dead wood, the depth of charring is limited by the drying depth. For example, the 1000-hr (40-day) depth of 0.1 m corresponds to only 100 yr of growth for western redcedar, so Gavin's inbuilt ages, $\lesssim$ 700 yr, must result from burning of snag interiors exposed by decay (Gavin, 2001; Schoennagel et al., 2004; Scott, 2010).

Charcoal from different forest environments will generally have different original distributions of inbuilt ages. The wetter climate of western Vancouver Island and the prevalence of rot-resistant western redcedar of $\sim$ 1000 yr age at Gavin's sites may lead to unusually large inbuilt ages. On the other extreme, the relatively dry climate of the Yellowstone Plateau in the Rocky Mountains has annual precipitation of 0.6–1.1 m (www.prismclimate.org) and forests dominated by lodgepole pine (*Pinus contorta var. latifolia* Engelm. ex. S. Wats). There, the greatest tree ages are generally < 300 yr, and mountain pine beetles kill many trees on cycles of 20–50 yr (Donato et al., 2013; Raffa et al., 2008; Romme and Despain, 1989).

Inbuilt ages in the Oregon Coast Range should generally lie between the above end members, due to shorter expected lifespans and greater snag decay rates at the Knowles Creek site relative to Gavin's site. Even if biomass production rates were similar at

the two sites, faster decay rates imply less dead biomass at the Knowles Creek site. Drier climate and dominance of Douglas-fir at the Knowles Creek site, then, imply dead wood in smaller volumes and with younger inbuilt ages by factors of 0.1 and 0.5, respectively, than on western Vancouver Island (Daniels et al., 1997; Gavin, 2001; Pabst et al., 2008).

Given the original inbuilt age distribution, potential charcoal transport distances may vary among age fractions. Much of the younger charcoal reaches the ground quickly, before soils are stabilized, so a disproportionate fraction of charcoal mobilized by rapid post-fire erosion and preserved in valley-floor deposits is relatively young. Much of the older charcoal may remain on boles until soils are stabilized, so a disproportionate fraction of charcoal preserved in near-surface hillslope soil is relatively old (Scott, 2010). Although transport processes differ, rapid post-fire erosion of predominantly young charcoal is common to the pairing of forest vegetation and steep terrain. For example, in both forests dominated by Douglas-fir in the Oregon Coast Range and ponderosa pine (*Pinus ponderosa* Dougl. ex P. & C. Laws.) in the Colorado Front Range, removal of ground cover, i.e., litter and understory vegetation, leads to rapid post-fire slope erosion, but by different processes, dry ravel and overland flow, respectively (Jackson and Roering, 2009; Larsen et al., 2009). Whereas shallow landslides generate debris flows in areas of low rainfall intensity such as the coastal ranges of Oregon, Washington, and British Columbia and the Western Cascade Range of Oregon, overland-flow erosion generates debris flows in much of the western U.S., whether in unvegetated areas or where fire has removed ground cover. Both types of debris flow largely entrain young charcoal from the last fire, but as overland flow generally erodes to shallower depths, charcoal content of runoff-generated debris flows may be more biased toward younger pieces (Cannon, 2001; Cannon et al., 2008; Jackson and Roering, 2009; Lancaster et al., 2012; McCoy et al., 2010; Meyer and Wells, 1997; Roering et al., 2003; Schmidt et al., 2001). At the Knowles Creek site, downstream sampling favors younger age fractions of the original inbuilt age distribution.

The interaction of charcoal (or other organic material) with transport processes and potential reservoirs determines potential inherited ages due to prior storage. Durability of transported material and destructiveness of transport processes determine likely transport distances and, hence, paths of charcoal that might be sampled at a given point in the channel network. Trapping efficiencies of and residence times in reservoirs along those paths and at the point of sampling determine the times of prior storage of sampled material. Inherited ages due to prior storage will increase with durability, trapping efficiencies, and residence times and decrease with destructiveness, and the potential for entrainment, transport, or deposition of charcoal pieces might vary among fractions with different prior storage durations.

For example, "burned soil surfaces" formed *in situ* (cf. Meyer et al., 1995; Pierce et al., 2004), delicate charred plant material unlikely to survive transport, or charcoal-rich near-surface soil layers that would be dispersed by transport (e.g., Gavin, 2001) all imply small or negligible transport distances and, thus, inherited ages due to prior storage upslope. Intensive sampling of such delicate materials in a small number of stratigraphic columns might essentially eliminate inherited ages. For example, Meyer et al. (1995) generally avoided durable material, but two pieces of rounded charcoal had mean ages 420 yr and 180 yr greater than an underlying conifer cone, their only age inversions among 90 samples from deposits in Yellowstone National Park, albeit with only 2 to 5 ages in most stratigraphic sections. At the other extreme, charcoal sampled from river channels by Blong and Gillespie (1978) was associated with rot-resistant and durable *Eucalyptus* L'Hér., and their large inherited ages apparently increased with greater downstream distance and smaller particle size.

The sites of Lancaster and Casebeer (2007) and Lancaster et al. (2010) lacked burned soil surfaces, and their study objectives excluded "minimally transported" materials like those sampled by Gavin (2001). Knowles Creek deposits contained various organic materials, but charred-wood charcoal was the only type found at all sampling locations. Since inbuilt ages at Knowles Creek may only be significant for a small number of samples with small inherited ages, the relative durability of charcoal suggests that upslope storage is the dominant control on inherited ages.

Given that control, the measured inherited age distributions reflect not only the strong association between fire and delivery of sediment to valley floors but also the variations in recurrence intervals of sediment evacuation along debris-flow runout paths. Both mechanisms would produce distributions peaked at zero but with large variations in thickness and length of the greater-age tail among the distributions for individual units. Debris flows scour their beds and thereby first entrain hillslope soil and colluvium, followed by colluvium and alluvium on steep valley floors. Material from a landslide initiation site includes not only recently raveled hillslope soil with abundant young charcoal but also the soil and charcoal gradually accumulated over the period since the previous failure ($\sim 10^3$ to 10^4 yr) (Montgomery et al., 2000; Reneau and Dietrich, 1991). At a point downstream of two landslide-prone sites, that period of gradual accumulation is, on average, half as long. Storage times on the steepest valley floors ($\gtrsim 10\%$) are therefore largely governed by debris-flow return periods that decrease systematically downstream in inverse proportion to the number of upstream debris-flow sources (Benda and Dunne, 1997b; Stock and Dietrich, 2006). However, stochasticity in valley-network structure and the timing of individual landslides, e.g., due to patchy and sporadic fires and other agents of tree mortality, will lead to similar stochasticity in ages of materials scoured by debris flows. Also, distributions of debris-flow runout lengths are typically right-skewed, and many debris flows form deposits in valleys with slopes $\gtrsim 30\%$ (Lancaster et al., 2001, 2003; Robison et al., 1999). We have observed that such steep-valley deposits, especially when indurated, may occasionally resist progressive, top-down scour and entrainment, cf. McCoy et al. (2012), by larger debris flows with longer runout lengths. Such resistance could produce substantial inherited ages, and this mechanism is probably not peculiar to the Oregon Coast Range.

Deposits sampled at Knowles Creek, and by Lancaster and Casebeer (2007) and Lancaster et al. (2010), sit near the downstream limit of debris-flow deposition and represent a strong bias toward greater runout lengths, shorter periods between scour, and entrainment of younger material (May and Gresswell, 2003; Stock and Dietrich, 2003). Among the Knowles Creek samples from debris-flow deposits, the greatest inherited age, ~ 10 kyr, is within the range of hollow-colluvium basal ages measured by Reneau and Dietrich (1991). The other five samples from the same unit have near-zero inherited ages, likely indicating either the aforementioned bias toward younger charcoal from the most recent fire, near-zero time since previous scour of the runout path, or both. (Table A.1 in supplement). Inherited ages for debris-flow deposits also appear to be more variable across the different units than for fluvial deposits; means and standard deviations for debris-flow units both span more than an order of magnitude. Some of the variation introduced through debris flows may be moderated due to mixing in the fluvial deposits.

5.2.2. *Differences Among Deposit Types*

For charcoal entering "final" storage in deposits at sampling locations, persistence of that charcoal in prior storage upstream is

apparently greatest for charcoal entering fluvial gravels. Conceptually, the inherited age PDF is the relative probability that charcoal of a given age will leave its prior storage location and enter final storage. The corresponding hazard rate function, $h_{I_f}(t)$, is the conditional probability of charcoal entering final storage with inherited age in the increment, $I_f \in [t, t + dt)$, given that the charcoal has already been in prior storage for that time, i.e., $I_f \geq t$. The complementary probability, $1 - h_{I_f}(t)$, is essentially the persistence of the charcoal in prior storage as a function of charcoal age. For an exponential PDF, the hazard rate is constant, $h_{I_f}(t) = 1/\overline{I_f}$, so that the probability of entering final storage is independent of time spent in prior storage. For a Weibull PDF, the hazard rate is a power law, $h_{I_f}(t) = (b_W/a_W)(t/a_W)^{b_W-1}$. For the best-fit shape parameters, $b_W < 1$, this rate is greater than the above constant rate for smaller t (e.g., $t < 830$ yr for fluvial gravel) and decreases with prior storage time. That is, charcoal in prior storage becomes more persistent with time. Increasing induration due to weathering, stabilization by vegetation, and increasing terrace height due to channel incision may all lead to increasing persistence with age and, moreover, might have similar effects on different deposit types.

Differences in probability of charcoal incorporation in the different deposit types might lead to different charcoal concentrations but not to differences in persistence in prior storage, except perhaps indirectly. Anecdotal observations suggest that charcoal concentrations in debris-flow deposits and fluvial fines are higher than in fluvial gravels. Relative to the fluvial transport of gravel, transport by debris flows is less frequent, and widespread debris-flow transport, such as occurs after fires, is rarer still. However, when widespread debris-flow transport does occur, typically soon after fire, younger charcoal is relatively abundant and mobile. Moreover, debris flows that reach valley floors like those along Knowles Creek do, almost without exception, produce deposits, usually large ones. In contrast, widespread gravel transport requires only mobile sediment and sufficient streamflow. Greater rates of fluvial gravel transport and deposition may be associated with debris-flow–driven supply, concomitant flooding, and recent fire, but relative to debris flows, greater fractions of fluvial gravel transport and deposition occur at times long after fire events. The stronger association between debris flows and fire and the relative abundance of young charcoal after fire might explain different persistence in storage prior to debris-flow vs. fluvial deposition, but differences in relative frequency and magnitude of transport events would suggest, counter to the evidence, even greater persistence prior to deposition of fluvial fines than of gravel.

To understand why that persistence is apparently greater for fluvial gravel than for both debris-flow deposits and fluvial fines and similar for the latter two, consider the conditions promoting not only transport but also deposition in the steep headwater streams of the study area. Whereas smaller, more numerous, leakier dams formed by fallen trees are generally sufficient to trap fluvial gravels, formation of lasting deposits of fluvial fines usually requires large dams, typically several meters high, formed by debris-flow deposits, (Lancaster and Grant, 2006). And impounded volumes can fill quickly: a supply of fine sediment equivalent to the average sediment yield over a 1-km^2 area could fill a typical accommodation space of 500 m^3 in 5 yr, and the supply associated with flooding and widespread debris flows following fire might fill that space within days. Such an association of deposits of fluvial fines with debris flows and, through them, with fire could explain why the inherited age distribution for fluvial fines is relatively similar to the distribution for debris-flow deposits. Conversely, the relatively weak association of fluvial gravel deposits with fire might explain the greater inherited ages of charcoal sampled from fluvial gravel.

5.3. Corrected Deposit Ages and Residence Times

While other materials (e.g., wood) may have different distributions of inherited ages than those of charcoal because of different potential for preservation and time spent incorporated in large boles, no inherited age data exist for these materials. We thus chose to correct residence times for all materials sampled by Lancaster and Casebeer (2007) and Lancaster et al. (2010) according to equation (5). Further study of inherited ages of other materials would provide greater insight into the effect of these ages on means of, and fits to, residence time distributions.

Inherited ages of charcoal samples taken from the Knowles Creek sites span a range similar to that of uncorrected deposit ages at the Bear Creek, Cedar Creek, and Golden Ridge Creek sites (Table 2; Tables A.2–A.5 in supplement), and mean inherited ages for the debris-flow, fluvial-fine, and fluvial-gravel facies in Knowles Creek are comparable to or greater than the uncorrected mean residence times of sediment at the other sites (Table 3, Fig. 4). Correction for inherited ages therefore reduces deposit ages substantially, but only the single greatest mean deposit age (16,660 yr at the time of sampling from fluvial gravel in mainstem Golden Ridge Creek; Table A.5 in supplement) is reduced by an amount equal to the mean inherited age for that facies. Most of the differences between corrected and uncorrected mean deposit ages are much less than the mean inherited ages for their respective facies, e.g., as little as 5 yr for an uncorrected deposit age of 11 yr (Table A.3 in supplement), because only inherited ages less than or equal to apparent deposit (sample) ages, T_d, contribute to conditional convolution in (5) (Fig. 5). PDFs of individual corrected deposit ages, T'_d, are flatter and broader than uncorrected PDFs, and thus convolution increases standard deviations, more so for greater deposit ages (Fig. 5; Tables A.2–A.5 in supplement). In contrast, for the residence time distributions, the effect of shifting all times toward zero outweighs the effect of increasing individual sample age standard deviations, so standard deviations for the normalized, corrected residence time distributions are smaller than for the uncorrected distributions (Table 1).

Correction for inherited age with equation (5) has small but significant effects on apparent age-dependence of the hazard rate function for sediment evacuation (11). Prior to correction, the "nearly exponential" gamma distribution of sediment residence times in lower Bear Creek implied that sediment evacuation probabilities decline only slightly with sediment age, e.g., by 35% from 1 to 1000 yr (Table 4), and sediment age and residence time distributions are nearly identical (Table 1). The gamma fit to the corrected residence time distribution, which has a slightly but significantly thicker tail (Table 4), implies a significant decrease in evacuation probability with age, e.g., by 81% from 1 to 1000 yr, so that sediment ages are significantly greater than residence times (95% confidence limits of mean residence time exclude the inferred mean sediment age) (Table 1). Although the best-fit power-law exponent actually increases with correction, we tend to discount this indication of a thinner tail, given other evidence and that the power law is fit only to $t > 2000$ yr (Fig. 6).

All other residence time distributions, both before and after correction for inherited age, indicate evacuation probabilities that are decreasing functions of sediment age, albeit decreasing more steeply after correction, as indicated by smaller gamma-distribution shape factors, a_Γ, and thus thicker tails at longer residence times. Although the changes are relatively small and do not necessarily represent major changes in interpretation of differences in the residence time distributions among sites, these changes are robust with respect to the uncertainties inherent in the estimation of true deposit ages from sampling at the Knowles Creek sites. These results imply that the corrected residence time distributions reflect

reservoir dynamics more accurately than do the uncorrected distributions.

6. Conclusions

For dating purposes, debris-flow deposits are associated with the smallest errors at the Knowles Creek site, followed by fluvial fines and fluvial gravels, but even charcoal samples from debris-flow deposits have a 50% chance of being off by more than 300 yr and a 10% chance of being off by more than 1500 yr.

Inherited ages derived from multiple sampling of the 14 depositional units in Knowles Creek have magnitudes similar to the uncorrected deposit ages found in the Bear, Cedar, and Golden Ridge Creek sites (Tables 1, 3), and the facies-specific mean inherited ages are comparable to mean residence times inferred from those deposit ages. However, correction for inherited ages does not reduce mean residence times by the magnitude of mean inherited ages, and most individual deposit ages are reduced by much less (Table 1; Tables A.2–A.5 in supplement). Rather than offsetting ages by simple subtraction, inherited ages are "subtracted" from the uncorrected deposit ages by convolution via (5), which is conditional on non-negative corrected ages. On average across all sites, corrected mean deposit ages are 29% younger than uncorrected, and the effects of correction on residence time distributions are comparable; on average, correction decreases mean residence times by 24%.

Whereas deposit age uncertainties arising from inherited age were previously unknown, the dramatically larger standard deviations of individual deposit age distributions introduced by correction with the convolution of (5) provide better informed and more accurate estimates of deposit age uncertainties. Correction also makes the distributions, and thus the 95% confidence limits representing the range of likely ages, highly left-skewed, so uncertainty increases asymmetrically toward younger age (Fig. 5). Although the bootstrapped confidence limits around corrected estimates of mean deposit ages are typically much smaller than the corrected standard deviations, those confidence limits reflect only the uncertainty in the estimate of the mean, and not the uncertainty in the estimate of the true deposit age.

In contrast to the large uncertainties in individual deposit ages revealed by inherited age correction, this correction introduces relatively small uncertainties to the inferred residence time distributions. Like the confidence intervals around the estimates of mean deposit ages, the bootstrapped confidence limits around corrected mean residence times and other diagnostic statistics are much smaller than the standard deviations of the component deposit age distributions, i.e., the $F_{T_{di}}$ values of (9). While these confidence intervals do not encompass all sources of uncertainty (e.g., due to sampling for residence times), the intervals do reflect the uncertainties arising from sampling for inherited age in particular and the correction process in general. These uncertainties are similar in magnitude to the 2σ ranges in the uncorrected calibrated deposit ages. Correction for inherited ages, then, provides better estimates of residence time distributions and reveals that inherited ages introduce essentially negligible additional uncertainty in those estimates, even though the magnitudes of the corrections are substantial. Corrected deposit ages and residence time distributions are robust with respect to sampling error because confidence intervals at younger inherited ages, which dominate the correcting convolution, are smaller than for greater ages. With this evident robustness, inherited age correction methods may be broadly applicable.

Among the valley-floor sediment reservoir sites, the Bear Creek reaches of Lancaster and Casebeer (2007) and Cedar Creek and Golden Ridge Creek tributary confluences of Lancaster et al. (2010), relative differences in reservoir dynamics implied by the residence time distributions are similar before and after correction, but correction does substantially modify our understanding of these sediment reservoirs. Correction thickens the tails of all the residence time distributions by similar amounts: gamma distribution shape factors decrease by 24.7% on average (23.7%–26.5%). Consequently, the ratio of mean sediment age and mean residence time, ranging from 1.03 to 1.80 before correction, increases by 21% on average (17.5%–24.7%), so that the corrected range is 1.21–2.18. Therefore, the degree of apparent age dependence of sediment evacuation probability increases substantially, and similarly, for all sites. So, whereas the previous results of Lancaster and Casebeer (2007) implied that fluvial evacuation of sediment at one of their two sites, lower Bear Creek, was age-independent, the corrected results reveal that evacuation at both sites of Lancaster and Casebeer (2007), as well as both sites of Lancaster et al. (2010), favors younger deposits.

Decreases in deposit age estimates with inherited age correction indicate that inherited ages may affect the results of diverse studies that depend on radiocarbon dating (e.g., seismology, paleofire ecology, and archeology), especially if only a few radiocarbon dates are made to suffice for age control of a long time series and contextual evidence of insignificant inherited ages is lacking. Although a similar study in a drier region with different vegetation and more intense storms than the Oregon Coast Range might reveal substantially smaller inherited ages, this remains somewhat speculative. Further study is warranted to elucidate controls on inherited ages of charcoal, and how these ages vary with dated material, depositional environment, and regional setting.

Acknowledgments

This paper is based upon work supported by the National Science Foundation under Grant Nos. EAR-0545768 and DEB-0333257 and a student grant from the Geological Society of America. J. Ame, C. Bergen, D. Bida, M. Diabat, and K. Hatcher assisted with sample collection and other field work. K. Motter assisted with acid-base-acid washing of charcoal samples at the Water Collaboratory at Oregon State University. D. Kennet provided laboratory facilities at the University of Oregon for sample combustion to produce carbon dioxide for radiocarbon dating. The NSF-Arizona AMS Laboratory dated the samples. This paper benefited from discussions with G. Grant, J. Jones, A. Meigs, J. Noller, F. Swanson, E. Thomann, and E. Underwood. A review by Grant Meyer resulted in significant improvement of the paper.

Appendix A. Supplementary data

Supplementary data related to this article can be found at http://dx.doi.org/10.1016/j.quascirev.2013.10.029.

References

Akciz, S. O., Grant Ludwig, L., Arrowsmith, J. R., 2009. Revised dates of large earthquakes along the Carrizo section of the San Andreas Fault, California, since A.D. 1310±30. Journal of Geophysical Research 114 (B01313), 1–16.

Anderson, S. P., Dietrich, W. E., Brimhall, G. H., 2002. Weathering profiles, mass-balance analysis, and rates of solute loss: Linkages between weathering and erosion in a small, steep catchment. Geological Society of America Bulletin 114 (9), 1143–1158.

Aubry, M.-P., Van Couvering, J. A., Christie-Blick, N., Landing, E., Pratt, B. R., Owen, D. E., Ferrusquía-Villafranca, I., 2009. Terminology of geological time: Establishment of a community standard. Stratigraphy 6 (2), 100–105.

Benda, L. E., Dunne, T., 1997a. Stochastic forcing of sediment routing and storage in channel networks. Water Resources Research 33 (12), 2865–2880.
Benda, L. E., Dunne, T., 1997b. Stochastic forcing of sediment supply to channel networks from landsliding and debris flow. Water Resources Research 33 (12), 2849–2863.
Benjamin, J., Cornell, C., 1970. Probability, Statistics, and Decision for Civil Engineers. McGraw-Hill, New York.
Blackard, J. A., Finco, M. V., Helmer, E. H., Holden, G. R., Hoppus, M. L., Jacobs, D. M., Lister, A. J., Moisen, G. G., Nelson, M. D., Riemann, R., Ruefenacht, B., Salajanu, D., Weyermann, D. L., Winterberger, K. C., Brandeis, T. J., Czaplewski, R. L., McRoberts, R. E., Patterson, P. L., Tymcio, R. P., 2008. Mapping U.S. forest biomass using nationwide forest inventory data and moderate resolution information. Remote Sensing of Environment 112 (4), 1658–1677.
Blong, R., Gillespie, R., 1978. Fluvially transported charcoal gives erroneous ^{14}C ages for recent deposits. Nature 271, 739–741.
Bolin, B., Rodhe, H., 1973. A note on the concepts of age distribution and transit time in natural reservoirs. Tellus 25, 58–62.
Bradley, D. N., Tucker, G. E., 2013. The storage time, age, and erosion hazard of laterally accreted sediment on the floodplain of a simulated meandering river. Journal of Geophysical Research: Earth Surface 118, 1–12.
Bush, M. B., Stillman, M. R., 2007. Amazonian exploitation revisited: Ecological asymmetry and the policy pendulum. Frontiers in Ecology and the Environment 5 (9), 457–465.
Cannon, S. H., 2001. Debris-flow generation from recently burned watersheds. Environmental & Engineering Geoscience 7 (4), 321–341.
Cannon, S. H., Gartner, J. E., Wilson, R. C., Bowers, J. C., Laber, J. L., 2008. Storm rainfall conditions for floods and debris flows from recently burned areas in southwestern Colorado and southern California. Geomorphology 96 (3–4), 250–269.
Costa, J. E., 1984. Physical geomorphology of debris flows. In: Costa, J. E., Fleisher, P. J. (Eds.), Developments and Applications of Geomorphology. Springer-Verlag, Berlin, pp. 268–317.
Daniels, L. D., Dobry, J., Klinka, K., Feller, M. C., 1997. Determining year of death of logs and snags of *Thuja plicata* in southwestern coastal British Columbia. Canadian Journal of Forest Research 27, 1132–1141.
Dietrich, W. E., Dunne, T., 1978. Sediment budget for a small catchment in mountainous terrain. Zeitschrift für Geomorphologie, Supplementbände 29, 191–206.
Dietrich, W. E., Dunne, T., Humphrey, N. F., Reid, L. M., 1982. Construction of sediment budgets for drainage basins. In: Swanson, F. J., Janda, R. J., Dunne, T., Swanston, D. N. (Eds.), Sediment Budgets and Routing in Forested Drainage Basins. No. PNW-141 in Forest Service General Technical Report. U.S. Department of Agriculture, Portland, Oregon, pp. 5–23.
Donato, D. C., Simard, M., Romme, W. H., Harvey, B. J., Turner, M. G., 2013. Evaluating post-outbreak management effects on future fuel profiles and stand structure in bark beetle-impacted forests of Greater Yellowstone. Forest Ecology and Management 303 (0), 160 – 174.
Efron, B., Tibshirani, R., 1993. An Introduction to the Bootstrap. Monographs on Statistics and Applied Probability. Chapman & Hall/CRC, Boca Raton.
Eriksson, E., 1971. Compartment models and reservoir theory. Annual Review of Ecology and Systematics 2, 67–84.
Franklin, J. F., Dyrness, C., 1973. Natural vegetation of Oregon and Washington. Forest Service General Technical Report PNW-8, U.S. Department of Agriculture.
Franklin, J. F., Hemstrom, M. A., 1981. Aspects of succession in the coniferous forests in the Pacific Northwest. In: West, D. C., Shugart, H. H., Botkin, D. B. (Eds.), Forest Succession: Concepts and Application. Springer-Verlag, New York, pp. 212–229.
Friquin, K. L., 2011. Material properties and external factors influencing the charring rate of solid wood and glue-laminated timber. Fire and Materials 35 (5), 303–327.
Frueh, W. T., 2011. Sediment reservoir dynamics on steepland valley floors: Influence of network structure and effects of inherited ages. Master's thesis, Oregon State University, Corvallis, Oregon.
Gavin, D. G., 2001. Estimation of inbuilt age in radiocarbon ages of soil charcoal for fire history studies. Radiocarbon 43 (1), 27–44.
Gavin, D. G., Brubaker, L. B., Lertzman, K. P., 2003. Holocene fire history of a coastal temperate rain forest based on soil charcoal radiocarbon dates. Ecology 84 (1), 186–201.
Heimsath, A. M., Dietrich, W. E., Nishiizumi, K., Finkel, R. C., 2001. Stochastic processes of soil production and transport: Erosion rates, topographic variation and cosmogenic nuclides in the Oregon Coast Range. Earth Surface Processes and Landforms 26 (5), 531–552.
Hua, Q., Barbetti, M., 2004. Review of tropospheric bomb C-14 data for carbon cycle modeling and age calibration purposes. Radiocarbon 46, 1273–1298.
Jackson, M., Roering, J. J., 2009. Post-fire geomorphic response in a steep, forested landscape: Oregon Coast Range, USA. Quaternary Science Reviews 28, 1131–1146.
Lancaster, S. T., Casebeer, N. E., 2007. Sediment storage and evacuation in headwater valleys at the transition between debris-flow and fluvial processes. Geology 35 (11), 1027–1030.
Lancaster, S. T., Grant, G. E., 2006. Debris dams and the relief of headwater streams. Geomorphology 82 (1–2), 84–97.
Lancaster, S. T., Hayes, S. K., Grant, G. E., 2001. Modeling sediment and wood storage and dynamics in small mountainous watersheds. In: Dorava, J. M., Montgomery, D. R., Palcsak, B. B., Fitzpatrick, F. A. (Eds.), Geomorphic Processes and Riverine Habitat. No. 4 in Water Science and Application. American Geophysical Union, Washington, D.C., pp. 85–102.
Lancaster, S. T., Hayes, S. K., Grant, G. E., 2003. Effects of wood on debris flow runout in small mountain watersheds. Water Resources Research 39 (6), 1–21.
Lancaster, S. T., Nolin, A. W., Copeland, E. A., Grant, G. E., 2012. Periglacial debris-flow initiation and susceptibility and glacier recession from imagery, airborne lidar, and ground-based mapping. Geosphere 8 (2), 417–430.
Lancaster, S. T., Underwood, E. F., Frueh, W. T., 2010. Sediment reservoirs at mountain stream confluences: Dynamics and effects of tributaries dominated by debris-flow and fluvial processes. Geological Society of America Bulletin 122 (11-12), 1775–1786.
Larsen, I. J., MacDonald, L. H., Brown, E., Rough, D., Welsh, M. J., Pietraszek, J. H., Libohova, Z., de Dios Benavides-Solorio, J., Schaffrath, K., 2009. Causes of post-fire runoff and erosion: Water repellency, cover, or soil sealing? Soil Science Society of America Journal 73 (4), 1393–1407.
Long, C. J., Whitlock, C., Bartlein, P. J., Millspaugh, S. H., 1998. A 9000-year fire history from the Oregon Coast Range, based on a high-resolution charcoal study. Canadian Journal of Forest Research 28 (5), 774–787.
Lowden, L. A., Hull, T. R., 2013. Flammability behaviour of wood and a review of the methods for its reduction. Fire Science Reviews 2 (4), 1–19.
Makhnin, O. V., 2010. Reliability and quality control. Lecture notes, New Mexico Institute of Mining and Technology.
URL http://infohost.nmt.edu/~olegm/484/
May, C. L., 2002. Debris flows through different forest age classes in the central oregon coast range. Journal of the American Water Resources Association 38 (4), 1097–1113.
May, C. L., Gresswell, R. E., 2003. Processes and rates of sediment and wood accumulation in headwater streams of the Oregon Coast Range, USA. Earth Surface Processes and Landforms 28 (4), 409–424.
McCoy, S. W., Kean, J. W., Coe, J. A., Staley, D. M., Wasklewicz, T. A., Tucker, G. E., 2010. Evolution of a natural debris flow: In situ measurements of flow dynamics, video imagery, and terrestrial laser scanning. Geology 38 (8), 735–738.
McCoy, S. W., Kean, J. W., Coe, J. A., Tucker, G. E., Staley, D. M., Wasklewicz, T. A., 2012. Sediment entrainment by debris flows: In situ measurements from the headwaters of a steep catchment. Journal of Geophysical Research: Earth Surface 117 (F03016), 1–25.
Meyer, G. A., Wells, S., 1997. Fire-related sedimentation events on alluvial fans, Yellowstone National Park, U.S.A. Journal of Sedimentary Research 67 (5), 776–791.
Meyer, G. A., Wells, S., Jull, A. J. T., 1995. Fire and alluvial chronology in yellowstone national park: Climatic and intrinsic controls on holocene geomorphic processes. Geological Society of America Bulletin 107, 1211–1230.
Miller, R. R., 2010. Is the past present? Historical splash-dam mapping and stream disturbance detection in the Oregon Coastal Province. Master's thesis, Oregon State University, Corvallis, Oregon.
Montgomery, D. R., Schmidt, K. M., Greenberg, H. M., Dietrich, W. E., 2000. Forest clearing and regional landsliding. Geology 28 (4), 311–314.
Nichols, G. J., Cripps, J. A., Collinson, M. E., Scott, A. C., 2000. Experiments in waterlogging and sedimentology of charcoal: results and implications. Palaeogeography, Palaeoclimatology, Palaeoecology 164 (1–4), 43–56.
Ohmann, J. L., Gregory, M. J., 2002. Predictive mapping of forest composition and structure with direct gradient analysis and nearest neighbor imputation in coastal oregon, usa. Canadian Journal of Forest Resources 32, 725–741.
Pabst, R. J., Goslin, M. N., Garman, S. L., Spies, T. A., 2008. Calibrating and testing a gap model for simulating forest management in the oregon coast range. Forest Ecology and Management 256, 958–972.
Personius, S. F., Kelsey, H. M., Grabau, P. C., 1993. Evidence for regional stream aggradation in the central Oregon Coast Range during the Pleistocene-Holocene transition. Quaternary Research 40, 297–308.

Pierce, J., Meyer, G., 2008. Long-term fire history from alluvial fan sediments: the role of drought and climate variability, and implications for management of Rocky Mountain forests. International Journal of Wildland Fire 17 (1), 84–95.

Pierce, J. L., Meyer, G. A., Jull, A. J. T., 11 2004. Fire-induced erosion and millennial-scale climate change in northern ponderosa pine forests. Nature 432 (7013), 87–90.

Pike, L. H., Rydell, R. A., Denison, W. C., 1977. A 400-year-old douglas fir tree and its epiphytes: biomass, surface area, and their distributions. Canadian Journal of Forest Research 7 (4), 680–699.

Raffa, K. F., Aukema, B. H., Bentz, B. J., Carroll, A. L., Hicke, J. A., Turner, M. G., Romme, W. H., 2008. Cross-scale drivers of natural disturbances prone to anthropogenic amplification: The dynamics of bark beetle eruptions. BioScience 58 (6), 501–517.

Reimer, P. J., Baillie, M. G. L., Bard, E., Bayliss, A., Beck, J. W., Blackwell, P. G., Ramsey, C. B., Buck, C. E., Burr, G. S., Edwards, R. L., Friedrich, M., Grootes, P. M., Guilderson, T. P., Hajdas, I., Heaton, T. J., Hogg, A. G., Hughen, K. A., Kaiser, K. F., Kromer, B., McCormac, F. G., Manning, S. W., Reimer, R. W., Richards, D. A., Southon, J. R., Talamo, S., Turney, C. S. M., van der Plicht, J., Weyhenmeyer, C. E., 2009. IntCal09 and Marine09 radiocarbon age calibration curves, 0–50,000 years cal BP. Radiocarbon 51 (4), 1111–1150.

Reneau, S. L., Dietrich, W. E., 1991. Erosion rates in the southern Oregon Coast Range: Evidence for an equilibrium between hillslope erosion and sediment yield. Earth Surface Processes and Landforms 16 (4), 307–322.

Robison, E. G., Mills, K. A., Paul, J., Dent, L., Skaugset, A., 1999. Storm impacts and landslides of 1996: final report. Forest Practices Technical Report 4, Oregon Department of Forestry.

Roering, J. J., Gerber, M., 2005. Fire and the evolution of steep, soil-mantled landscapes. Geology 33, 349–352.

Roering, J. J., Schmidt, K. M., Stock, J. D., Dietrich, W. E., Montgomery, D. R., 2003. Shallow landsliding, root reinforcement, and the spatial distribution of trees in the oregon coast range. Canadian Geotechnical Journal 40, 237–253.

Romme, W. H., Despain, D. G., 1989. Historical perspective on the Yellowstone fires of 1988. BioScience 39 (10), 695–699.

Schmidt, K. M., Roering, J. J., Stock, J. D., Dietrich, W. E., Montgomery, D. R., Schaub, T., 2001. The variability of root cohesion as an influence on shallow landslide susceptibility in the oregon coast range. Canadian Geotechnical Journal 38, 995–1024.

Schoennagel, T., Veblen, T. T., Romme, W. H., 2013/09/24 2004. The interaction of fire, fuels, and climate across Rocky Mountain forests. BioScience 54 (7), 661–676.

Scott, A. C., 2010. Charcoal recognition, taphonomy and uses in palaeoenvironmental analysis. Palaeogeography, Palaeoclimatology, Palaeoecology 291 (1–2), 11–39.

Sigman, K., 1999. A primer on heavy-tailed distributions. Queueing Systems 33, 261–275.

Sollins, P., Cline, S. P., Verhoeven, T., Sachs, D., Spycher, G., 1987. Patterns of log decay in old-growth Douglas-fir forests. Canadian Journal of Forest Research 17, 1585–1595.

Spies, T. A., Franklin, J. F., Thomas, T. B., 1988. Coarse woody debris in douglas-fir forests of western oregon and washington. Ecology 69 (6), 1689–1702.

Stock, J. D., Dietrich, W. E., 2003. Valley incision by debris flows: Evidence of a topographic signature. Water Resources Research 39 (4), 1089.

Stock, J. D., Dietrich, W. E., 2006. Erosion of steepland valleys by debris flows. Geological Society of America Bulletin 118, 1125–1148.

Sullivan, A., Ball, R., 2012. Thermal decomposition and combustion chemistry of cellulosic biomass. Atmospheric Environment 47, 133–141.

Sullivan, A. L., Ellis, P. F., Knight, I. K., 01 2003. A review of radiant heat flux models used in bushfire applications. International Journal of Wildland Fire 12 (1), 101–110.

Swanson, F. J., 1981. Fire and geomorphic processes. In: Proceedings, Fire Regimes and Ecosystems Conference. No. WC-20 in General Technical Report. U.S. Department of Agriculture Forest Service, Washington, D.C., pp. 401–420.

Sweeney, K. E., Roering, J. J., Almond, P., Reckling, T., 2012. How steady are steady-state landscapes? using visible–near-infrared soil spectroscopy to quantify erosional variability. Geology 40 (9), 807–810.

Telford, R. J., Heegard, E., Birks, H. J. B., 2004. The intercept is a poor estimate of a calibrated radiocarbon age. The Holocene 14, 296–298.

Tornqvist, T., de Jong, A., Oosterbaan, W. A., der Borg, K., 1992. Accurate dating of organic deposits by AMS ^{14}C measurement of macrofossils. Radiocarbon 34 (3), 566–577.

Tucker, G. E., 2004. Drainage basin sensitivity to tectonic and climatic forcing: implications of a stochastic model for the role of entrainment and erosion thresholds. Earth Surface Processes and Landforms 29 (2), 185–205.

Tucker, G. E., Bras, R. L., 2000. A stochastic approach to modeling the role of rainfall variability in drainage basin evolution. Water Resources Research 36 (7), 1953–1964.

Wells, F. G., Peck, D. L., 1961. Geologic map of Oregon west of the 121st Meridian. Miscellaneous Geologic Investigations Map I-325, U.S. Geological Survey, Washington, D.C.

Western Regional Climate Center, September 16, 2013. RAWS monthly summary time series, Goodwin Peak, Oregon, 1985–2013. Web page. URL http://www.raws.dri.edu/